Elucidating the Downstream Position and Functional Role of SFK Activation After CagA Phosphorylation in *Helicobacter pylori* Infection

Ramanayake Mudiyanselage Ashansa Pamodhi

Ramanayake

Department of Applied Life Sciences

The Graduate School

Yonsei University

Elucidating the Downstream Position and Functional Role of SFK Activation After CagA Phosphorylation in *Helicobacter pylori* Infection

Directed by Professor Jeong-Heon Cha

The Doctoral Dissertation Submitted to

the Department of Applied Life Sciences,

the Graduate School of Yonsei University

in partial fulfillment of the requirements

for the degree of Doctor of Philosophy in Applied Life Science

Ramanayake Mudiyanselage Ashansa Pamodhi Ramanayake

June 2025

Elucidating the Downstream Position and Functional Role of SFK Activation After CagA Phosphorylation in *Helicobacter pylori* Infection

This certifies that the Dissertation of Ramanayake Mudiyanselage Ashansa Pamodhi Ramanayake is approved.

_____

Thesis Supervisor: Prof. Jeong-Heon Cha

_____

Thesis Committee Member: Prof. Yun-Jung Yoo

_____

Thesis Committee Member: Prof. Ki-Woo Kim

_____

Thesis Committee Member: Prof. Na-Young Song

_____

Thesis Committee Member: Prof. Sang Sun Yoon

Department of Applied Life Sciences

The Graduate School

Yonsei University

June 2025

ACKNOWLEDGEMENT

First and foremost, I would like to express my sincere gratitude to my supervisor, Prof. Cha Jeong-Heon, for his unwavering guidance and support throughout my research journey. It has been an honor to be mentored by such an exceptional scientist, whose expertise and dedication have profoundly shaped my academic and professional growth. Despite the challenges along the way, you have not only guided me in research but also instilled in me the ability to multitask, manage pressure, and navigate highly demanding situations.

I am also deeply grateful to Dr. Rasika Illeperuma for providing me with this invaluable opportunity to be a part of this research environment and to pursue my studies at one of the world's top-ranked universities. Your support has played a pivotal role in shaping my academic path, and I truly appreciate the trust and encouragement you have extended to me.

I would also like to extend my heartfelt gratitude to Dr. Kim, Jinmoon, an exceptional senior whose unwavering support throughout my Ph.D. journey making it truly invaluable. Despite meeting only once and being based in the U.S., your guidance has had a profound impact on my understanding of scientific principles and experimental techniques. I deeply appreciate your willingness to assist me whenever I reached out, never hesitating to provide insightful advice and prompt responses. Your support has meant more to me than words can express. Also, I would like to extend my gratitude to Prof. Yun-Jung Yoo for her kind words that kept me motivated and for her continued encouragement and belief in my

potential, which helped me stay focused and resilient during the last few semesters of my research journey.

I would like to express my sincere appreciation to my seniors, Prof. Kim Aeri, Dr. Jing Lai, Dr. Kim Myeong-ah, Dr. Angulmaduwa, Dr. Noh Eui-jeong, and Seo Jiwon Sem, for their generous support and valuable insights throughout my research. A heartfelt thank you to Prof. Kim, Aeri for your constant kindness and encouragement, which lifted me during difficult times and truly inspired me to keep going and strive for better. Dr. Lai, Jing, and Dr. Kim, Myeong-ah, your guidance was always a great help during challenging experiments, and I feel very fortunate to have had your academic support. To Dr. Angulmaduwa, thank you for being a constant source of both academic and emotional support. You were not just a senior, but like an elder brother whose support meant a great deal. I am also profoundly grateful to Jiwon Sem for always being such kind and approachable senior who supported me with most of the administrative work and technical challenges.

I'm truly grateful to my friends Dr. Adasooriya, Dilan, So-hee, Hsu, Shiqi, and Kaweesha for being by my side throughout this journey. Your constant support, kindness, and presence made all the difference, especially during the moments when I felt overwhelmed. You reminded me that I wasn't alone, and your encouragement gave me the strength to keep moving forward. I genuinely couldn't have made it through without each of you. Also, I am grateful to my lab colleagues, Min-seo, Jae yun, Dowon, Roshan, and Sung-kyong for

their considerate and friendly nature. Your respectful attitude and positive presence helped foster a supportive atmosphere in the lab, making it a more comfortable place to work.

Finally, I would like to express my deepest and most heartfelt gratitude to my beloved family, my parents, my husband, my sister, and my brother, for being my unwavering source of strength and love throughout this journey. Even though we were often miles apart, your presence was always felt. You stood by me unconditionally, listened patiently to my countless worries, and lifted me when things felt too heavy to carry alone. Your belief in me never wavered, and knowing you were there made all the difference.

A special thank you goes to my dear husband, Kasun. You have been my anchor and my safe space through it all. You listened to every frustration, comforted me during my lowest moments, and reminded me to keep going when I felt like giving up. No one understands the depth of this journey better than you, and I genuinely cannot imagine having made it through without your love, patience, and quiet strength.

With utmost honor, I would like to dedicate my thesis to my dearest Dad and Mom. From the very beginning, you instilled in me the values of resilience, integrity, and hard work. It was your dream to see me reach great heights, and every step I've taken has been with that dream in my heart. This achievement is as much yours as it is mine, and I hope I've made you proud.

TABLE OF CONTENTS

Part I

Part II

LIST OF FIGURES

LIST OF TABLES

ABSTRACT

Elucidating the Downstream Position and Functional Role of SFK Activation After CagA Phosphorylation in *Helicobacter pylori* Infection

Ramanayake Mudiyanselage Ashansa Pamodhi Ramanayake

Department of Applied Life Sciences

The Graduate School

Yonsei University

(Directed by Professor Jeong-Heon Cha)

Helicobacter pylori is a gastric pathogen closely associated with various gastric diseases. Its key virulence factor, the oncoprotein CagA, is delivered into gastric epithelial cells via a type IV secretion system, where it undergoes tyrosine phosphorylation and triggers signaling pathways that induce cell elongation ("hummingbird phenotype"). While Src family kinases (SFKs) have been identified as the main kinases mediating CagA phosphorylation, this study re-evaluates their role by examining the interplay between CagA phosphorylation, SFK activation, and downstream cellular effects.

The *Helicobacter pylori* strain G27, as well as AGS and MKN28 gastric cancer cell lines were used to conduct the study. Our findings revealed that SFK activation was entirely inhibited at 0.5 μM PP2 without significantly affecting CagA phosphorylation, cell elongation, or IL-8 induction, indicating that SFK is not essential for these processes. At higher PP2 concentrations, both CagA phosphorylation and cell elongation were reduced in a dose-dependent manner. Immunofluorescence and FACS analyses revealed that PP2 treatment decreased *H. pylori* binding to AGS cells, potentially accounting for the observed effects. Infections with Δ*cagA* and phosphorylation-resistant *cagA*-EPISA strains failed to activate SFK, suggesting that SFK activation occurs downstream of CagA phosphorylation. We demonstrated that *H. pylori*-mediated SFK activation is regulated via the Shp2-Raf-Mek-Erk pathway by employing specific siRNA and inhibitors. SFK inhibition did not impact ERK activation and IL-8 induction. However, wound healing and transwell invasion assays demonstrated that SFK inhibition significantly impairs *H. pylori*-induced wound

healing and cell invasion, underscoring a specific role for SFK in modulating host cell motility during infection.

Our study propose that SFK activation occurs downstream of CagA phosphorylation, potentially via ERK pathway activation. This suggests that alternative kinases may be responsible for CagA phosphorylation, offering new insights into the molecular mechanisms of *Helicobacter pylori* pathogenesis. Although SFK was dispensable for CagA phosphorylation, cell elongation, ERK activation, and IL-8 induction, it governed the migratory and invasive responses induced by *H. pylori*. These findings highlight a previously under-recognized but essential function of SFK in regulating host cell motility during infection.

Keywords: *Helicobacter pylori*, SFK Activation, CagA Phosphorylation, Cell elongation, IL-8 induction, Shp2, Raf, Mek, Erk, Cell migration and invasion

1. Introduction

Helicobacter pylori inhabits the stomach of 43.9% of the adult global population and accounts for almost 90% of distal gastric cancers [1-3]. This bacterium has been implicated in multiple gastric pathologies, including chronic gastritis, peptic ulcers, gastric adenocarcinoma, and mucosa-associated lymphoid tissue (MALT) lymphoma [4,5]. Notably, *H. pylori* infection substantially elevates the risk of developing cancer, holding the fourth spot in worldwide cancer mortality, responsible for approximately 768,000 deaths annually [6,7]. Recognizing the significance of this association, the International Agency for Research on Cancer (IARC) classified *H. pylori* as a Group 1 carcinogen [8].

The majority of *H. pylori* strains contain the cag pathogenicity island (*cag*PAI), which comprises approximately 32 genes, including the *cagA*. A functional type IV secretion system (T4SS) that encoded by this genomic element delivers the effector oncoprotein CagA into host cells [9]. Once inside the host cells, CagA is localized to the host cell membrane, where the tyrosine residue of the Glu-Pro-Ile-Tyr-Ala (EPIYA) motif is phosphorylated [10,11] by host cell kinases. Following phosphorylation, CagA engages with the Src homology region 2-containing phosphatase 2 (Shp2), forming a complex, leading to the deregulation of Shp-2 and prolonging the activation of the Raf-Mek-Erk pathway [12,13].

The extracellular signal-regulated kinase (Erk) pathway is predominantly activated by receptor tyrosine kinases (RTKs) in response to extracellular stimuli. Upon activation,

RTKs stimulate a signaling cascade involving adaptor proteins that facilitate the conversion of Ras to its active form. Activated Ras then triggers the activation of Raf kinases (A-Raf, B-Raf, and C-Raf), which phosphorylate and activate the MAPK kinases Mek1 and Mek2. These, in turn, phosphorylate and activate Erk1 and Erk2, leading to various downstream events such as cell scattering [14], elongation [15], and inflammatory [16,17] cellular responses as a result of *H. pylori* infection. Phosphorylated CagA induces an elongation phenotype in gastric epithelial cells [18]. Furthermore, it has been previously demonstrated that the cell elongation phenotype occurs via Shp2-mediated Ras-independent Erk activity [19,20] .

It was previously assumed that members of the Src family kinases (SFKs), which include nine non-receptor tyrosine kinases such as Blk, Fgr, Fyn, Hck, Lck, Lyn, Src, Yes, and Yrk, played a central role in mediating CagA phosphorylation [21,22]. They exert broad regulatory influence over cellular behavior [23], and the catalytic activity of SFKs are strictly regulated by two tyrosine residues: Y416 and Y527. Phosphorylation of Y416 equivalent in the activation loop favors the active conformation of the catalytic center, enabling SFK to act as a kinase. In the inactive state, Y527 equivalent is phosphorylated, and dephosphorylation of Y527 by protein tyrosine phosphatases (PTPs) such as PTPα activates SFK by disrupting the auto-inhibitory conformation [23].

Activation of SFKs and the ERK signaling pathway has been extensively implicated in cytoskeletal remodeling, Focal adhesion dynamics, IL-8-mediated inflammatory responses, and, importantly, the regulation of cancer cell migration and invasion in various cellular

contexts. Exposure to *H. pylori* triggers robust migratory responses in host cells, suggesting a critical role for these signaling pathways in *H. pylori*-mediated pathogenesis. Upon infection, translocated CagA undergoes tyrosine phosphorylation, leading to the activation of downstream effectors such as focal adhesion kinase (FAK) and paxillin, which are key regulators of cytoskeletal reorganization and cell motility [24,25]. Additionally, activation of Erk [26] upon *H. pylori* infection is involved with SFK signaling and contributes to enhanced migratory behavior.

Despite extensive research on *H. pylori* pathogenesis, the precise role of Src family kinases in CagA phosphorylation and downstream signaling remains incompletely understood. Although SFKs have been widely implicated in mediating CagA phosphorylation, emerging evidence suggests the involvement of alternative kinases and pathways. Furthermore, the specific contribution of SFKs to other infection-induced cellular responses, such as host cell migration and invasion, remains unclear. This study aims to clarify the functional relevance of SFK activation in *H. pylori*-infected gastric epithelial cells. By employing optimized experimental approaches and dissecting key signaling events, we provide insights into the CagA phosphorylation-dependent novel signaling hierarchy underlying SFK activation and its role in modulating host cell behavior during *H. pylori* infection.

2. Materials and Methods

2.1. *H. pylori* Strains and Culture

This study mainly employed *Helicobacter pylori* strain G27 wild-type, a CagA-deficient mutant (G27 Δ*cagA*), a phosphorylation-resistant variant (G27 *cagA*-EPISA), and a GFP-expressing derivative (G27/pGFP). The G27 wild-type strain was initially developed in the laboratory of Stanley Falkow and is currently maintained in the Merrell lab collection. This strain has originally been recovered from an Italian patient diagnosed with duodenal ulcer and has been widely used for the CagA-related studies since the strain is capable of effectively translocating CagA into gastric epithelial cells and robustly undergoes phosphorylation [27-30]. The growth of all *H. pylori* strains was carried out using the protocol established by Gunawardhana et al. (2017) [31]. Briefly, Columbia blood agar (BD) supplemented with 5% defibrinated horse blood, selective antibiotics, and β-cyclodextrin was used to grow *H. pylori* strains at 37℃ under microaerophilic conditions. *H. pylori* liquid cultures were maintained in Brucella broth (BD) supplemented with 10% fetal bovine serum (FBS, Gibco) and 10 μg/mL vancomycin, and incubated at 37°C under microaerophilic conditions with constant shaking at 120 rpm.

2.2. Gastric Cancer Cell Culture

The AGS and MKN28 gastric cancer cell lines obtained from the American Type Culture Collection (ATCC) were used in this study. AGS cells originate from human gastric

adenocarcinoma, while MKN28 cells represent a well-differentiated tubular adenocarcinoma isolated from a lymph node metastasis [32]. Cells were cultured in DMEM (Gibco) containing 10% heat-inactivated FBS and 1% penicillin-streptomycin (Gibco), and grown at 37°C under 5% CO_2 in a humidified incubator.

2.3. Treatment of PP2 / CI-1040 and *H. pylori* Infection

A total of 4×10^5 AGS cells were distributed into each well of a 6-well plate containing 2 ml of DMEM with 10% fetal bovine serum. Once the cells reached approximately 80% confluence, they were subjected to serum starvation in DMEM without FBS for 2 hours, followed by treatment with the SFK inhibitor PP2 for 30 minutes. Then, cells were infected with *H. pylori* at a multiplicity of infection (MOI) of 100 for 5 hrs for the short-time infection and 24 hours for the long-time infection. CI-1040 inhibitor treatment was carried out following 2 hours of serum starvation for 24 hours before the *H. pylori* infection.

2.4. Western Blot Analysis

After rinsing with phosphate-buffered saline (PBS), cells were disrupted in a lysis buffer containing PMSF, sodium orthovanadate (NaVO3), and a protease inhibitor cocktail (Cell Signaling Technology). Whole cell lysates were denatured, resolved on 10 % SDS-PAGE gels, and transferred onto PVDF membranes (Millipore).

This study utilized the following primary antibodies: anti-p-SFK (Y416), MEK1/2, ERK1/2, and phospho-ERK1/2 (all 1:1000; Cell Signaling Technology), as well as

phosphotyrosine (pY99), total SFK (SC 18), total CagA, Urease A, and GAPDH (all 1:1000; Santa Cruz Biotechnology). Tris-buffered saline containing 0.1% Tween 20 (TBST) and 3% bovine serum albumin (BSA; GenDepot) was used to dilute antibodies, allowing for simultaneous blocking and primary antibody incubation overnight at 4℃. Following incubation, membranes were incubated with horseradish peroxidase (HRP)-conjugated goat anti-rabbit or goat anti-mouse IgG secondary antibodies (Santa Cruz Biotechnology) for 1 hour at room temperature. It was carried out following three consecutive washes with TBST. Protein bands were detected using an enhanced chemiluminescence (ECL) solution (Advansta) according to the manufacturer's instructions.

2.5. Transient Transfection of Small Interfering RNA (siRNA)

Listed below are utilized in this work. For A-Raf knockdown, a pool of three target-specific siRNAs was employed, while single siRNA molecules were used for all other gene silencing experiments. AGS cells were seeded in 6-well plates at a density of 3×10^5 cells per well in DMEM containing 10% FBS. Once the cells reached approximately 80% confluence, they were serum-starved for 2 hours before transfection. Lipofectamine 2000 (Invitrogen) reagent was used to conduct siRNA transfection according to the manufacturer's protocol. 50 or 100 pM final siRNA concentrations were employed to achieve the knock down. Six hours post-transfection, the fresh medium was added to maintain 10% FBS. After 24 hours of transfection, media was replaced with fresh DMEM

containing 10% FBS. After 48 hours of transfection, cells were infected with *H. pylori* at an MOI of 100 for the indicated time points.

Table 1. The siRNA used is this study

Target	Sequences (5′ → 3′)
NT	AAA CCG UCG AUU UCA CCC GGG
A-Raf	1. CGA GAU CUC AAG UCU AAC A 2. GCU UCC AGU CAG ACG UCU A 3. GGA CUC CUC UCU UUC UUC A
B-Raf	AAA GAA UUG GAU CUG GAU CAU
C-Raf	UAG UUC AGC AGU UUG GCU A
Mek1	GCU UCU AUG GUG CGU UCU ACA
Mek2	UGG ACU AUA UUG UGA ACG AGC
Erk1	AAC UUG UAC AGG UCA GUC U
Erk2	AAU AAG UCC AGA GCU UUG G

2.6. IL-8 induction

4×10^5 AGS cells were seeded per well of a 6-well plate using 2 ml of DMEM supplemented with 10% FBS. After 22 hours of seeding, the cells were serum-starved for 2 hours in serum-free DMEM. Following this, PP2 was applied for 30 minutes to assess its effect. Then, cells were infected with *H. pylori* at an MOI of 100 for 5 hours for the short-time infection and 24 hours for the long-time infection. After the infection, culture supernatant was used to determine the concentration of secreted IL-8 using an enzyme-linked immunosorbent assay using Human IL-8 ELISA MAX™ (BioLegend).

2.7. Cell Elongation Assay

Growing AGS cells, serum starvation, and the PP2 treatment were conducted as described in the IL-8 induction assay. Then, the cells were infected with *H. pylori* at an MOI of 100 for 5 hours. Post *H. pylori* infection, 4% paraformaldehyde was used to fix the cells for microscopy. Cell elongation pictures were taken from CKX41 inverted microscope and DP20 microscope camera (Olympus) under ×200 magnification. Five pictures were taken from each well of three independent replicates. The scale bar was set, and cell elongation induced by 100 cells from each well was measured using ImageJ v1.47 (National Institutes of Health, Bethesda, MD). Cells protruding 20 μM or more were defined as elongated cells [14,33].

2.8. Immunofluorescence Assay for *H. pylori* Attachment

Autoclaved 12 mm × 7.5 mm glass slides were placed in a 24-well plate, washed with PBS, and coated with 250 μL poly-L-lysine overnight at 4℃. After washing with PBS, 20 μL of 2% gelatin was added to each well and incubated at 37℃ for 10 minutes. Slides were washed 2-3 times with PBS before seeding cells at a density of 1-2 × 10^5 cells per well. PP2 treatment and *H. pylori* infection were carried out once the cells reached 80% confluence.

For time-course analysis of *H. pylori* attachment, cells were infected at a MOI of 25 for varying time points. To assess the effect of PP2 on *H. pylori* binding, cells were pre-treated with varying concentrations of PP2 for 30 minutes, followed by infection at a MOI of 25 for 2 hours.

After the infection cells were fixed with 3-4% formaldehyde at 4℃ for 10-30 minutes and then washed with PBS and permeabilized using 0.1% Triton X-100 in PBS for 3-5 minutes. To reduce non-specific binding, cells were blocked with 3% BSA in PBS for 1 hour at room temperature. For actin visualization, cells were incubated with a β-actin primary antibody (Santa Cruz Biotechnology) for 2 hours at room temperature. After three washes with TBST, cells were incubated with an Alexa Fluor 594-conjugated anti-mouse IgG secondary antibody. Coverslips were mounted using Vectashield mounting medium and imaged using a Zeiss LSM700 confocal microscope. Actin filaments were detected using 594 nm excitation, while *H. pylori* attachment was visualized via green fluorescence.

2.9. FACS Analysis

AGS cells pretreated with different PP2 concentrations for 30 minutes were infected with *H. pylori* strain G27/pGFP for 2 hours. An MOI of 25 was employed for bacterial infection. After infection, PBS-washed cells were detached using 0.05% trypsin-EDTA (Gibco). Afterward, cells were subjected to a 15-minute fixation at room temperature using 4% paraformaldehyde, followed by three sequential PBS washes to remove any residual fixative. To evaluate GFP expression, AGS cells were subjected to flow cytometric analysis using the BD FACSCanto II system (BD Biosciences), and the collected fluorescence data were subsequently interpreted using FlowJo software (Tree Star Inc.). GFP-positive cell percentages were used as an indicator of the degree of *H. pylori* adherence to AGS cells.

2.10. Wound healing assay

Cells were seeded in six-well plates at a density of 1.5×10^6 cells per well and allowed to adhere for 22 hours. Once the cells achieved 100% confluency, cells were serum-starved in plain DMEM for 2 hours.

Subsequently, a linear wound was created using a 10 μl pipette tip. Cells were then treated with either PP2 or DMSO (vehicle control) for 2 hours, followed by infection with *H. pylori* at a multiplicity of infection (MOI) of 100 for 16 hours. Representative images were captured at 0 hours and 16 hours of infection, and wound closure was quantified using ImageJ software. For each wound, three representative regions were imaged, and within each region, three distinct locations were assessed for wound healing. Wound closure was

determined by measuring the difference between the initial wound width and the width after 16 hours of infection. Cell migration was presented relative to the uninfected control. Data is expressed as the mean ± SD of three independent experiments.

2.11. Transwell invasion assay

Cell invasion was assessed using a Transwell invasion assay (SPL, Pocheon, South Korea), which consisted of 12-well cell culture inserts with 8-μm pore size membranes. Matrigel (Corning, NY, USA) was diluted in plain DMEM at a 1:10 ratio, and 100 μL of the diluted Matrigel was applied to the upper surface of the membrane. The Matrigel was allowed to polymerize for 2 hours at 37°C in a cell culture incubator. After polymerization, 1×10^5 cells were seeded into the Matrigel-coated inserts (upper chamber), while DMEM containing 10% FBS (without antibiotics) was added to the bottom chamber as a chemoattractant. Cells were allowed to settle for 6 hours, and the cells in the upper chamber were infected with *H. pylori* at a multiplicity of infection (MOI) of 100. Following 16 hours of infection, non-invaded cells and the remaining matrigel in the upper chamber were removed using a cotton swab. The invaded cells on the underside of the membrane were then fixed with 4% paraformaldehyde for 15 minutes and stained with 1% crystal violet. Each experimental category was triplicated and five representative images were captured from each replicate. Cell invasion was quantified using ImageJ software. Three independent experiments contributed to express data as mean ± SD.

2.12. Statistical Analysis

All results are presented as the mean with corresponding standard deviation (SD). To assess statistical differences, one-way ANOVA was conducted using GraphPad Prism version 8. For multiple group comparisons, Tukey's post hoc test was employed. Differences were considered statistically significant at a P-value < 0.05.

3. Results

Part I

3.1.1. Effects of SFK inhibition on CagA phosphorylation.

To assess whether *H. pylori* infection induces SFK activation, *H. pylori* G27 strain was used to infect AGS cells at four different time points. SFK activation was evaluated by immunoblotting. Activation of SFKs was detectable as early as 1 hour post-infection, with a more robust increase observed at 5 hours, indicating a time-dependent enhancement of SFK activation upon infection. Subsequently, we treated AGS cells with the SFK inhibitor PP2 to evaluate SFK activation and CagA phosphorylation to understand the effect of SFK inhibition on phosphorylation of CagA. First, AGS cells were pretreated with five different PP2 concentrations for 30 minutes, and then were infected with the *H. pylori* strain G27 for 5 hours. Post *H. pylori* infection, SFK activation, and CagA phosphorylation were determined by western blot. G27 infection strongly activates the SFKs after 5 hours of infection. Treatment with one μM PP2 almost completely inhibited SFK activation, and the rest of the PP2 concentrations also achieved SFK inhibition levels similar to 1 μM PP2. At 1 μM concentration CagA phosphorylation was only slightly reduced. However, CagA phosphorylation was dose-dependently decreased with increasing PP2 concentrations (Fig. 1).

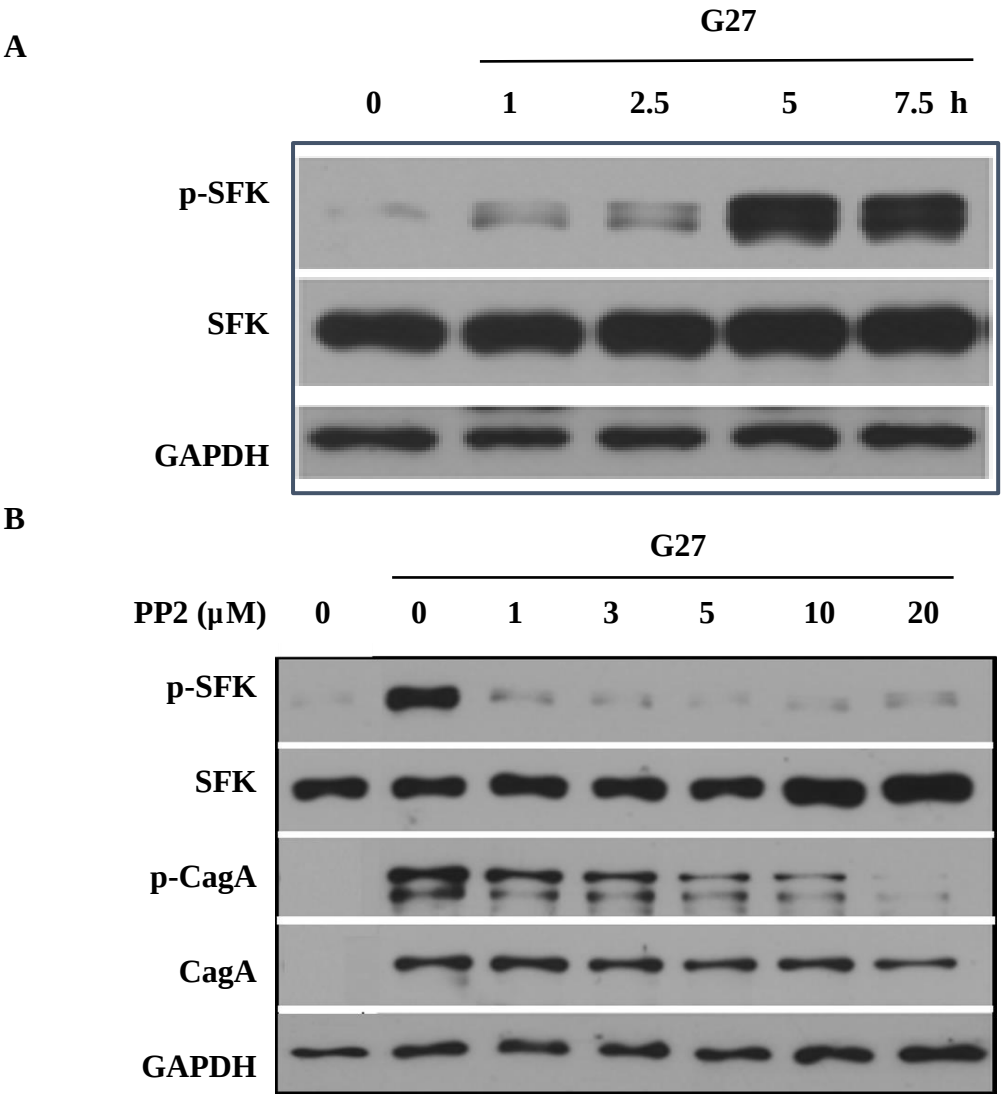

Figure 1. Effects of SFK inhibition on CagA phosphorylation. (A) AGS cells were infected with G27 for different time courses, and the SFK activation was determined. (B) AGS cells were pretreated with five different concentrations of PP2 and subsequently infected with *H. pylori* strain G27 (MOI-100) for 5 hours. Cell lysates were immunoblotted for phosphorylated SFK (p-SFK), total SFK (SFK), phosphorylated CagA (p-CagA), total CagA (CagA), and Glyceraldehyde-3-phosphate dehydrogenase (GAPDH). GAPDH was used as the loading control.

3.1.2. Effects of SFK inhibition on Cell elongation.

Phosphorylation of CagA triggers the characteristic elongation of cells, which is also known as the hummingbird phenotype. Therefore, we investigated the dose-dependent effect of SFK inhibitor PP2 on cell elongation phenotype. The percentage of elongated cells was calculated in different PP2 concentrations. Consistent with the pattern observed in CagA phosphorylation level, one μM PP2 did not significantly alter the percentage of elongated cells. However, the percentage of cell elongation gradually decreased with increasing PP2 concentration, demonstrating a significant reduction in the elongation phenotype. This observation prompted further refined experiments to explore the relationship between SFK and CagA phosphorylation (Fig. 2).

A

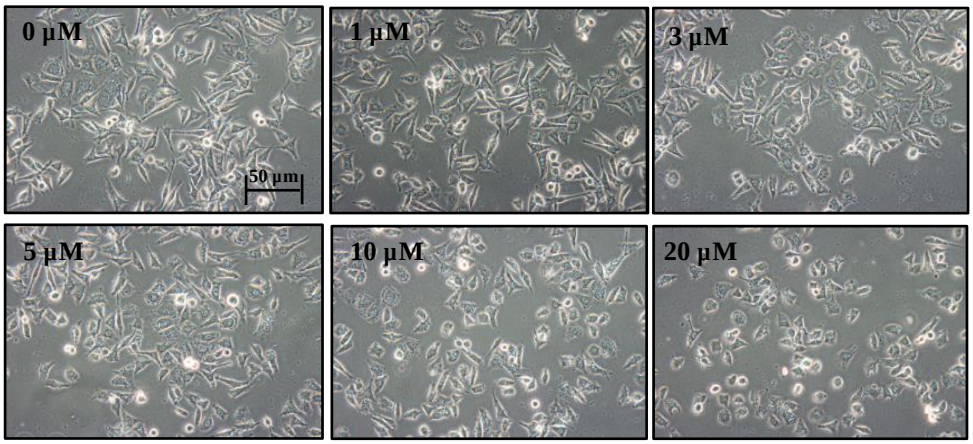

B

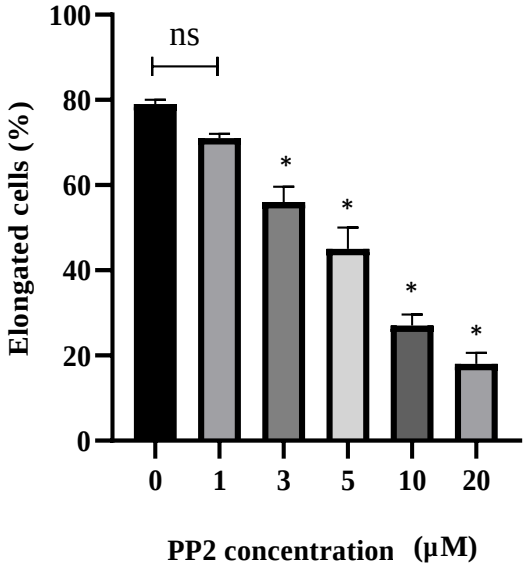

Figure 2. Effects of SFK inhibition on Cell elongation. (A) Micrographs were taken under ×200 magnification, and the (B) percentage of elongated cells was quantified at different PP2 concentrations. Using the Image J Software, lengths of the cell protrusions were measured, and cells with protrusions similar to or longer than 20 μm were considered as elongated cells. Values represent the mean ± standard deviation of three independent experiments conducted in triplicate. **P* < 0.01 indicates a significant difference compared to the PP2 untreated control. ns, not significant.

3.1.3. Inhibitory effects of PP2 on Total CagA and UreaseA expression.

UreA and CagA are markers used to indicate the amount of *H. pylori* attached to AGS cells after infection. To evaluate the effect of increasing PP2 concentrations on these markers, three different concentrations of PP2 were employed, and the levels of SFK activation, CagA phosphorylation, total CagA, and UreA levels were determined at five different time points of G27 infection. Upon G27 infection of AGS cells, SFK activation was progressively increased. Similarly, UreA, total CagA, and phospho-CagA expression levels were increased, indicating enhanced bacterial attachment and CagA translocation to AGS cells over time. In line with previous findings, treatment with 1 μM PP2 effectively suppressed SFK activation, while mildly reducing CagA phosphorylation. This effect was more evident during the early stages of infection. Interestingly, both UreA and total CagA levels showed a slight decrease relative to the untreated control. PP2 concentrations exceeding 1 μM resulted in a comparable level of SFK inhibition. However, at these PP2 concentrations (3 μM and 10 μM), a clear dose-dependent reduction was observed in UreA,

total CagA, and phosphorylated CagA. GAPDH indicated that the protein loading was consistent across samples. Based on the observations, we suggest that PP2 induces an inhibitory effect on CagA translocation by impairing *H. pylori* binding to AGS cells.

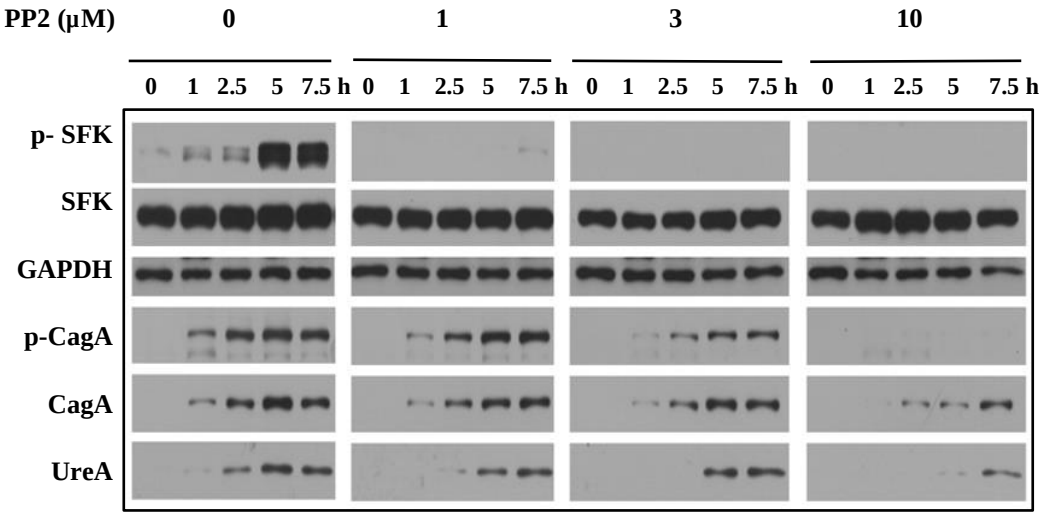

Figure 3. Inhibitory effects of PP2 on Total CagA and UreaseA expression. AGS cells were pretreated with three different concentrations of PP2 and then infected with G27 (MOI-100) for 5 different time points. Total cell lysates were immunoblotted for p-SFK, SFK, p-CagA, CagA, Urease A (UreA), and GAPDH. UreA was used as the infection control.

3.1.4. Temporal Dynamics of *H. pylori* Adherence to AGS Cells.

The temporal profile of bacterial attachment to AGS cells was evaluated by employing the G27 strain expressing Green Fluorescent Protein (G27/pGFP). Initially, we observed bacterial binding to AGS cells over time without PP2 treatment. Infection of AGS cells with G27/pGFP was performed at an MOI of 25, followed by incubation for various durations, and an immunofluorescence assay was conducted to visualize the bacterial binding to AGS cells. The cell cytoskeleton was stained using a β-actin antibody. As expected, *H. pylori* attachment to AGS cells gradually increased over time (Fig. 4A). Aligning with the pattern observed in *H. pylori* attachment, both CagA expression and subsequent phosphorylation were progressively increased over the time course of infection (Fig. 4B).

A

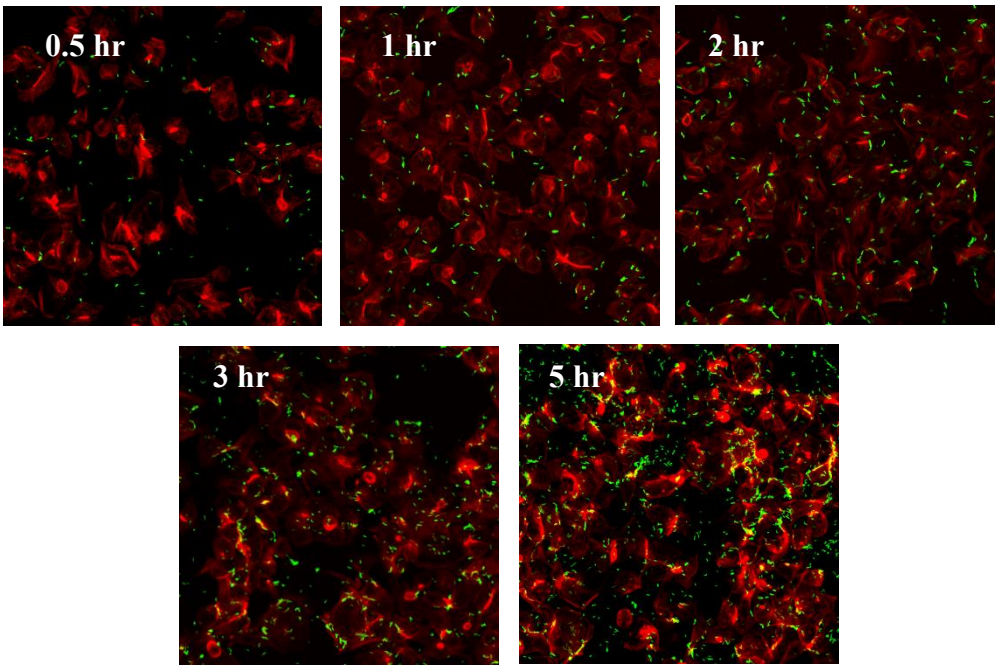

B

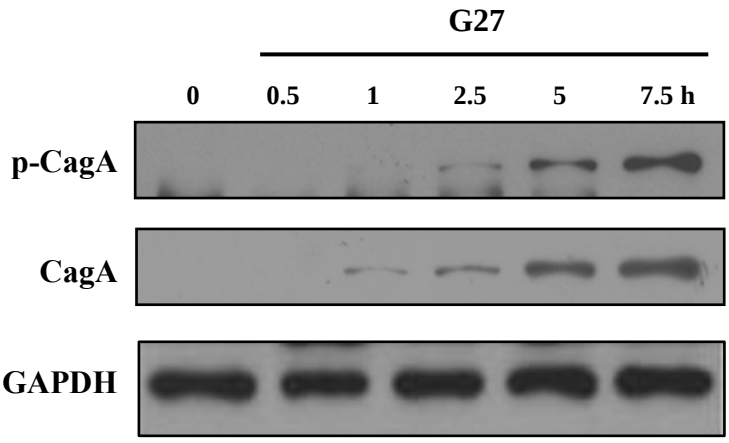

Figure 4. Temporal Dynamics of *H. pylori* Adherence to AGS Cells. (A) AGS cells were infected with the G27/pGFP strain (MOI-25) for different time points, and *H. pylori* attachment over time was determined by confocal microscopy. *H. pylori* and actin were stained with green and red fluorescence, respectively. Each image represented three independent experiments. (B) Total CagA expression and subsequent phosphorylation were determined by immunoblot.

3.1.5. Effects of increasing PP2 concentrations on *H. pylori* binding to cells- Immune Fluorescence Assay.

Subsequently, we treated the cells with four different PP2 concentrations and infected them with *H. pylori* for 2 hours to assess the impact of SFK inhibition on *H. pylori* binding to AGS cells. At ×400 magnification, microscopic images revealed that *H. pylori* adhered to cell-cell junctions, and bacterial binding to the cells gradually decreased with increasing PP2 concentrations. Representative images are shown here (Fig. 5A). We quantified *H. pylori* binding by calculating the ratio of *H. pylori* to cell number. Exposure to PP2 at both 1 μM and 10 μM concentrations led to a substantial decrease in bacterial binding. However, *H. pylori* attachment to AGS cells was not significantly affected by 0.1 and 0.5 μM PP2 concentration (Fig. 5B).

A

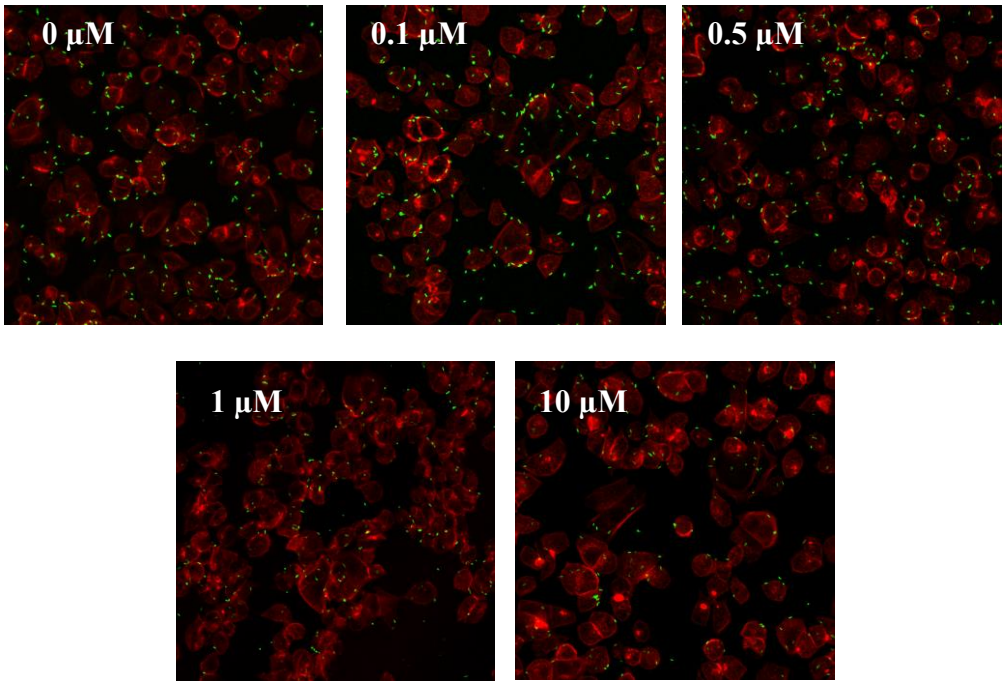

B

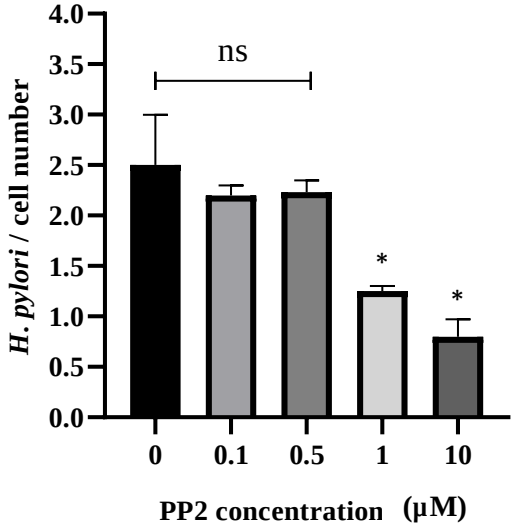

Figure 5. Effect of PP2 on bacterial attachment- Immunofluorescence assay. (A) AGS cells pretreated with different PP2 concentrations were infected with G27/pGFP (MOI-25) for 2 hours. *H. pylori* attachment to AGS cells was determined by confocal microscopy. (B) *H. pylori* attachment to AGS cells was quantified by the *H. pylori* /cell number ratio. Values represent the mean ± standard deviation of three independent experiments conducted in triplicate. $*P < 0.05$ indicate the significant difference compared to PP2 untreated control.

3.1.6. Effects of increasing PP2 concentrations on *H. pylori* binding to cells- FACS Analysis.

To reinforce the observations made via immunofluorescence, we performed flow cytometry to quantify bacterial attachment. Red peak shows the GFP intensity associated with infected cells, and grey peak shows the baseline auto-fluorescence of uninfected AGS cells (Fig. 6).

As expected, the GFP signal intensity associated with AGS cells exhibited a dose-dependent decline following PP2 treatment, with a marked reduction observed between 1 µM and 10 µM concentrations (Fig. 7). While percent attachment remained relatively constant up to 0.5 µM PP2, a significant decrease was detected from 1 µM PP2, further supporting the idea that PP2 shows dose-dependent impairment of bacterial binding.

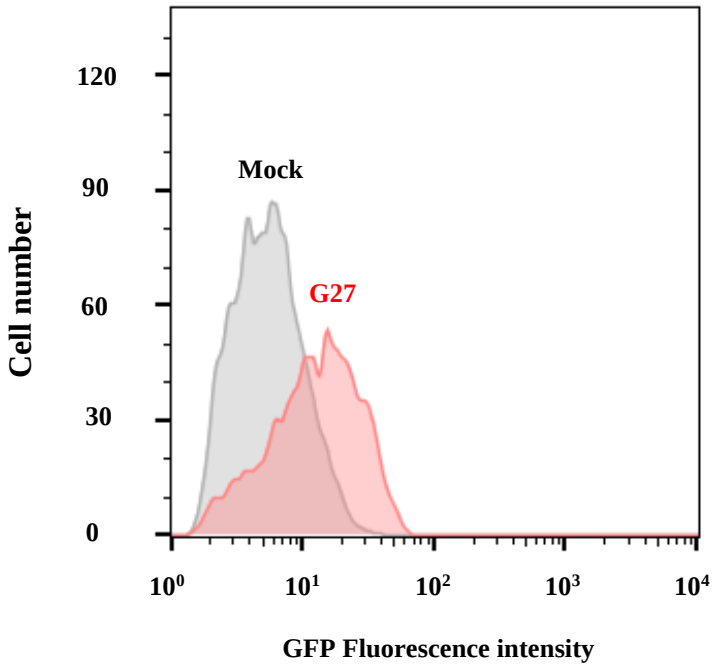

Figure 6. Fluorescence signal in infected vs. uninfected AGS cells. (A) AGS cells with or without G27/GFP infection were scrapped to isolate single cells. Single-cell suspension was subjected to FACS analysis to determine the intensity of fluorescence emission. A smooth histogram shows the intensity of fluorescence emission of AGS cells with or without G27/GFP infection. Mean GFP fluorescence intensity (MFI) is shown on the x-axis (log scale) and the number of AGS cells in each fluorescence class on the y-axis (linear scale).

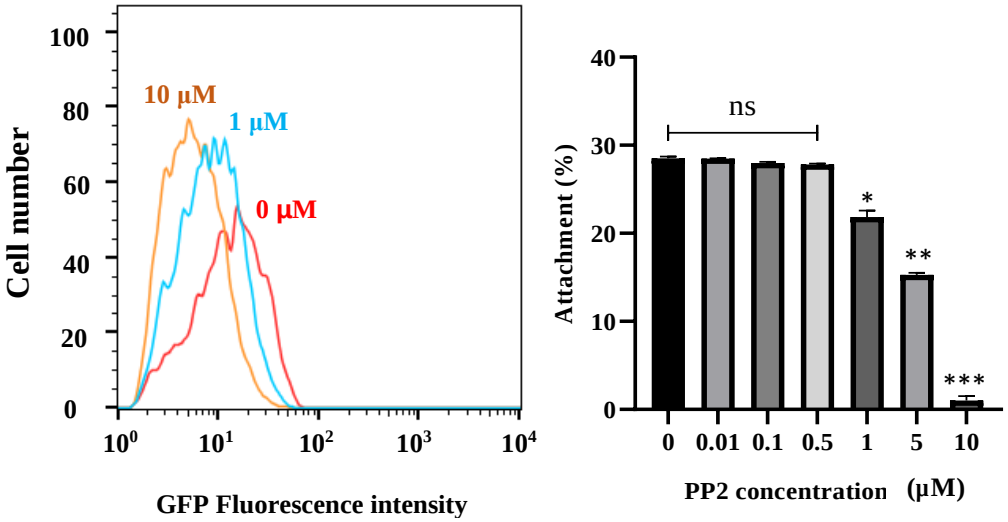

Figure 7. Effect of PP2 on bacterial attachment-FACS analysis. (A) AGS cells pretreated with different concentrations of PP2 were subjected to FACS analysis. The red peak represents MFI associated with cells treated with DMSO without PP2. The blue peak represents the MFI of cells with 1 μM PP2. The yellow peak represents the MFI associated with cells treated 10 μM PP2. (C) Percent attachment in different PP2 concentrations were plotted against the different PP2 concentration. Values represent the mean ± standard deviation of three independent experiments conducted in triplicate. *P < 0.05; **P < 0.01; ***P < 0.001 indicate the significant difference compared to PP2 untreated group.

3.1.7. Impact of SFK inhibition on ERK activation and IL-8 induction.

H. pylori attachment and interaction of T4SS with gastric epithelial cells activate signal transduction mechanisms within the host cell, particularly the MAPK pathway [16]. Additionally, CagL, positioned on the exterior of the T4SS, facilitates interaction with host cell integrins [34], triggering integrin-mediated signaling. Previous studies have shown that IL-8 induction by *H. pylori* at an early stage is primarily dependent on the T4SS. Moreover, CagA translocation to epithelial cells via the T4SS prolongs Erk activation. To rule out the impact of SFK inhibition and the impact of attenuated bacterial binding on *H. pylori*-induced Erk activation and IL-8 induction, we treated AGS cells with 1, 3, and 10 μM PP2, and the Erk activation and IL-8 induction were determined over a different time course of infection. One μM PP2 did not strongly impair the Erk activation by G27. However, Erk activation was gradually decreased with increasing PP2 concentrations (Fig. 8A). G27 infection with 1 and 3 μM PP2 treatment showed comparable IL-8 secretion levels to infection alone. However, treatment with 10 μM PP2 significantly reduced the IL-8 induction after 5 hours of infection (Fig. 8B).

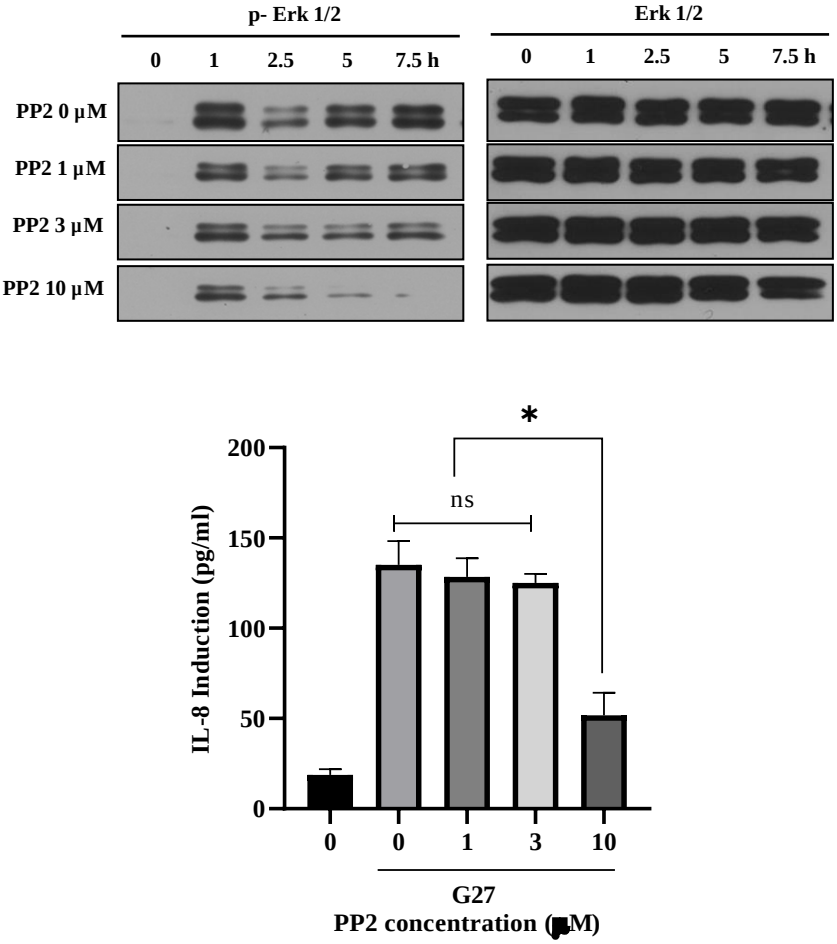

Figure 8. Effects of SFK inhibition on Erk activation and IL-8 induction. (A) AGS cells were treated with 1, 3 and 10 μM of PP2, and phosphorylated Erk (p-Erk) and total Erk (Erk) were immunoblotted at different time course of *H. pylori* infection (MOI-100). (B) IL-8 secretion was determined 5 hours post-infection at three different PP2 concentrations. *$P < 0.05$ indicate the significant difference compared to PP2 untreated group.

3.1.8. Ruling out the optimum PP2 concentration inhibiting SFK activation without impairing the *H. pylori* adherence.

To identify the minimal effective concentration of PP2 capable of inhibiting SFK activation without compromising *H. pylori* adherence, 0.1 and 0.5 μM PP2 concentrations were used to treat. These concentrations were specifically chosen based on preliminary findings indicating that these two concentrations do not significantly interfere with bacterial attachment to the host cells. At 0.1 μM, PP2 did not effectively inhibit SFK activation in response to G27 infection. In contrast, treatment with 0.5 μM PP2 resulted in a marked suppression of SFK activation. Importantly, despite robust inhibition of SFK, CagA phosphorylation levels at 0.5 μM PP2 remained comparable to those observed in untreated infected cells. This finding provides strong evidence that SFK activity is not required for CagA phosphorylation (Fig. 9).

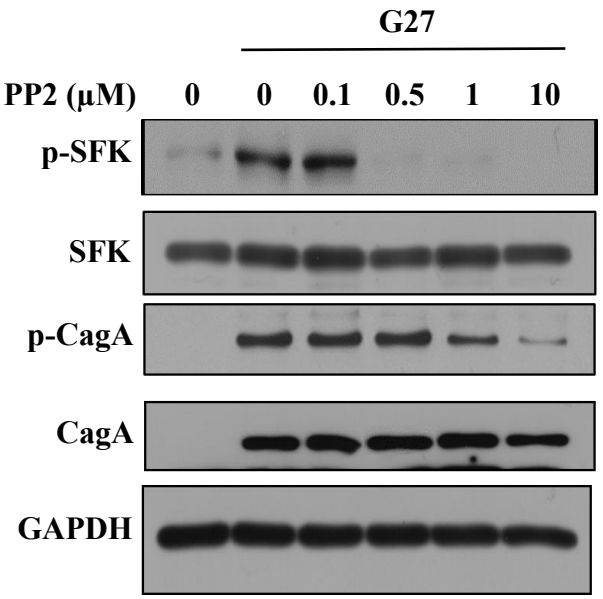

Figure 9. PP2-Mediated Inhibition of SFK: A Dose-Response Analysis. AGS cells were pretreated with 0.1, 0.5, 1, and 10 μM of PP2 and subsequently infected with *H. pylori* strain G27 (MOI-100) for 5 hours. Cell lysates were immunoblotted for p-SFK, SFK, p-CagA and CagA and GAPDH.

3.1.9. Effect of SKF inhibition on CagA phosphorylation and resulting cell elongation of the MKN28 cell line.

To characterize the MKN28 cell line for CagA phosphorylation and the associated cell elongation phenotype, we treated MKN28 cells with 0.5 μM PP2 and infected the cells with G27 for 6 hours. Subsequently, the effect of SFK inhibition on CagA phosphorylation and cell elongation was examined. As expected, treatment with 0.5 μM PP2 effectively suppressed SFK activation. However, CagA phosphorylation remained unaffected, and cell elongation occurred at levels comparable to the control group. Using an alternative cell line, we further supported the idea that SFKs are dispensable for CagA phosphorylation and the induction of the cell elongation phenotype (Fig. 10).

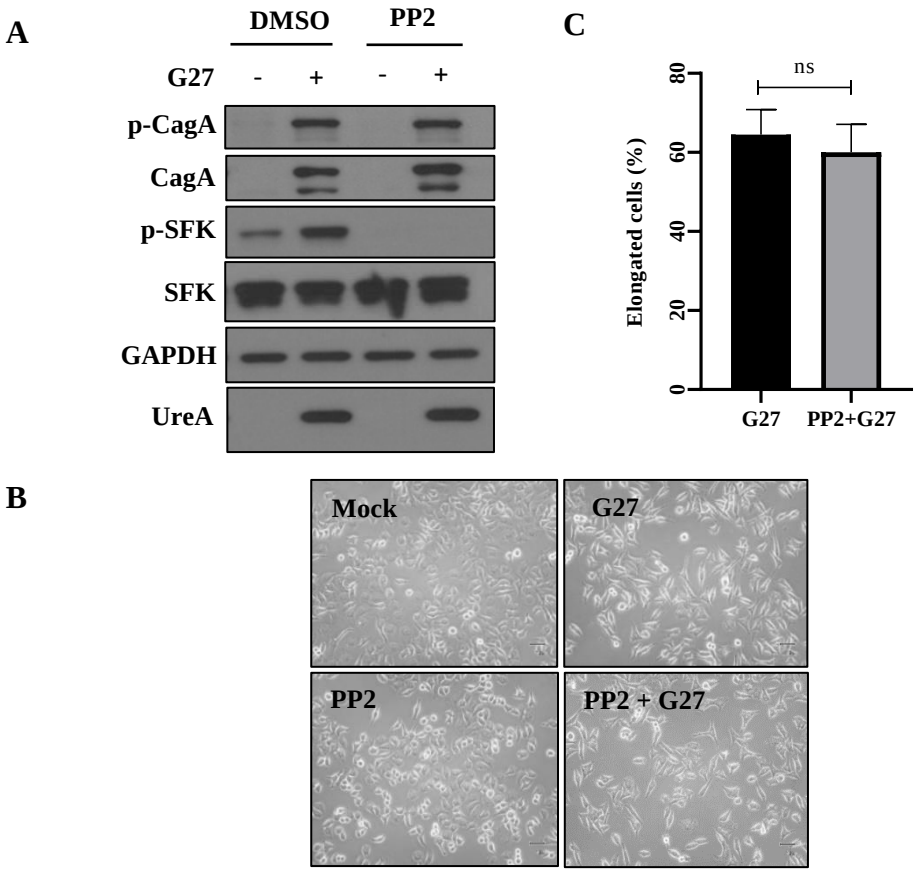

Figure 10. Characterizing MKN28 cell lines for cell elongation and CagA phosphorylation upon SFK inhibition. (A) MKN28 cells pre-treated with 0.5 μM PP2 for 30 minutes, followed by *H. pylori* infection for 6 hours. SFK activation and CagA phosphorylation were analyzed by immunoblotting. (B) Representative images of MKN28 cell morphology were captured at ×200 magnification to assess cell elongation. (C) The percentage of elongated cells was quantified using image J software.

3.1.10. Effect of SFK inhibition on *H. pylori*-mediated IL-8 induction.

Among the genes induced by *H. pylori* infection in gastric epithelial cells, IL-8 is reported to show the highest level of upregulation [35]. Also, the secretion of IL-8 by *H. pylori* is strain and time-dependent, and mostly, the IL-8 induced at a later time point shows a significant contribution from CagA [36]. Studies involving CagA transfection indicate that IL-8 induction mediated by CagA requires both SFK and Erk signaling pathways [37]. Therefore, we determined whether *H. pylori*-induced IL-8 induction is dependent on SFK by employing 0.5 μM PP2. Both early and late time IL-8 inductions were measured by ELISA assay. G27 infection significantly induced IL-8 compared to the uninfected control. However, the SFK inhibition by 0.5 μM PP2 treatment did not alleviate the IL-8 induction at both early and late time points (Fig. 11), indicating that SFK activation is not essential for the *H. pylori*-mediated IL-8 induction.

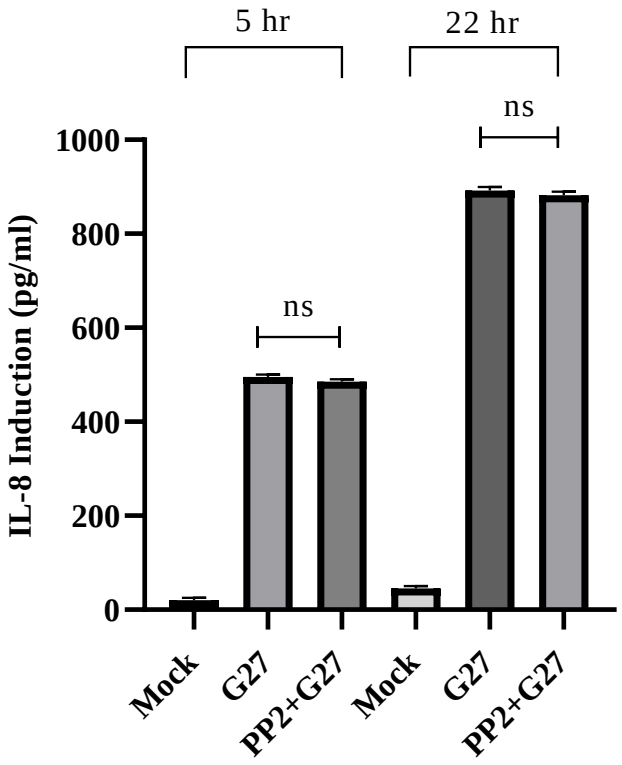

Figure 11. Effect of SFK inhibition on *H. pylori*-mediated IL-8 induction. AGS cells were pretreated with 0.5 μM of PP2 for 30 minutes prior to the infection with G27. Short term IL-8 induction was determined after 5 hours of infection and long term IL-8 induction was determined after 22 hours of infection.

Part II

3.2.1. *H. pylori*-induced SFK activation as a downstream phenomenon of CagA phosphorylation.

To rule out the relationship between CagA and SFK activation, we infected AGS cells with G27 wild type, *cagA*-deleted (Δ*cagA*), and phosphorylation-resistant (*cagA*-EPISA) strains. The *cagA*-EPISA mutant strain was genetically engineered by changing all four tyrosine residues of the EPIYA-A, B, and two EPIYA C motifs to serine residues. *H. pylori* CagA phosphorylation in AGS cells induces cell elongations, which is widely known as the hummingbird phenotype.

G27 wild-type CagA underwent phosphorylation upon translocation, inducing strong cell elongations. Following the CagA phosphorylation pattern, G27 wild type shows progressive SFK activation over the course of infection. G27 Δ*cagA* neither expresses the CagA protein nor induces cell elongation. G27 strain expresses the CagA protein and does not undergo phosphorylation upon translocation. As a result, G27 *cagA*-EPISA strain fails to induce the hummingbird phenotype. To our surprise, both Δ*cagA, and cagA*-EPISA strains fail to fully activate SFKs suggesting that SFK activation mainly occurs downstream of CagA phosphorylation (Fig. 12). This observation revealed that not only the presence of CagA but also its tyrosine phosphorylation is required for full SFK activation.

A

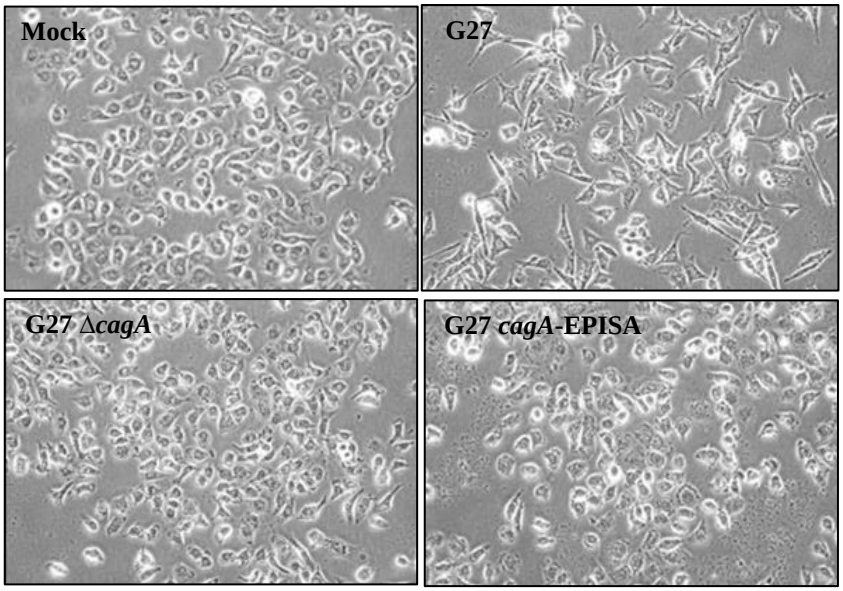

B

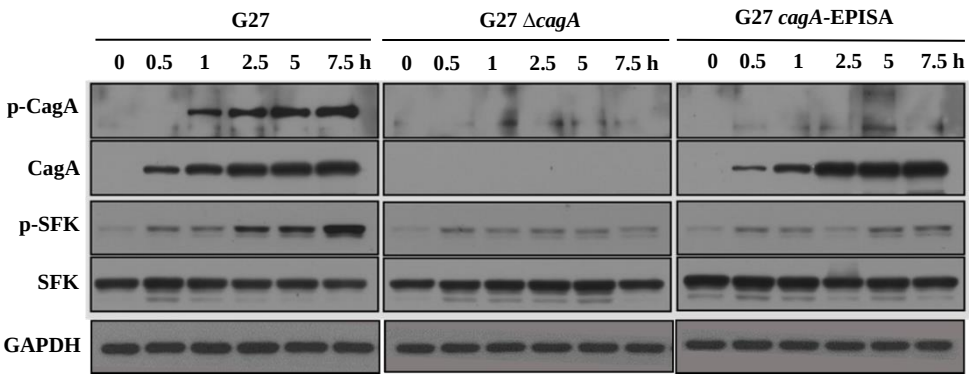

Figure 12. *H. pylori*-induced SFK activation is dependent on CagA phosphorylation. (A) Micrographs were taken after 5 hours of *H. pylori* infection at ×200 magnification. (B) AGS cells were infected for different time points with G27 wild type and isogenic Δ*cagA* and *cagA*-EPISA strains. p-CagA, CagA, p-SFK and SFK were immunoblotted to determine the CagA phosphorylation and SFK activation.

3.2.2. Effect of Shp2 inhibition on *H. pylori*-induced SFK activation.

In previous data, we showed that the SFK activation is a phenomenon primarily dependent on CagA phosphorylation. It has been previously found that Shp2 is an immediate intracellular target of the tyrosine phosphorylated CagA, and interaction of phosphorylated CagA and Shp2 is an essential component for the induction of the hummingbird phenotype [12,38]. As an immediate downstream target of phosphorylated CagA, we next investigated whether Shp2 is crucial for SFK activation. Specific siRNA was employed to knock down the Shp2 expression. SHP2 siRNA strongly reduced the Shp2 expression. Shp2 knockdown dramatically impaired the SFK activation by G27, indicating that Shp2 is crucial for inducing the SFK activation by G27 (Fig. 13).

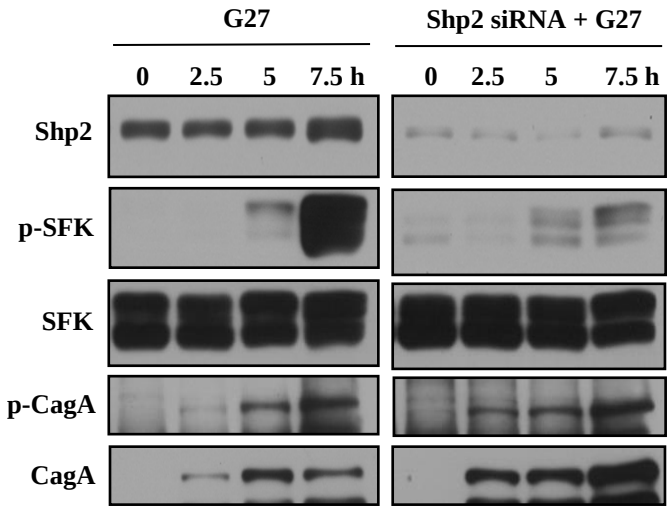

Figure 13. Shp2 as a key mediator of *H. pylori*-induced SFK activation. AGS cells were transfected with 100 pM Shp2 siRNA. Forty-eight hours post transfection, cells were infected with G27 for varying time periods, and Shp2 expression (Shp2) and SFK activation was determined by immunoblot.

It was previously found that the interaction of phosphorylated CagA with Shp2 activate the Shp2-Erk axis [38,39]. Additionally, the CagA-induced Shp2-mediated morphogenetic response has been described as a Ras-independent phenomenon. Therefore, we investigated other Erk pathway-specific molecules such as Raf, Mek, and Erk to determine the necessity of the Shp2-Raf-Mek-Erk axis on *H. pylori*-induced SFK activation.

3.2.3. Effect of Raf inhibition on *H. pylori*-induced SFK activation

The Raf family comprises three different isoforms; A-Raf, B-Raf, and C-Raf that mediate signal transduction through the formation of homo- or heterodimers. To find out the necessity of each Raf isoform, single siRNA transfection was carried out to knock down the expression of individual Raf isoform at a time. The siRNA transfection almost entirely blocked Raf expression (Fig. 14A). Knockdown of A-Raf alone substantially impaired SFK activation at 5 hours post-infection, and knockdown of B-Raf alone strongly impaired the SFK activation beyond 2.5 hours of infection. However, knockdown of C-Raf alone substantially impaired overall SFK activation throughout the infection time points. These observations suggested that all three isoforms show differential roles in *H. pylori*-induced SFK activation (Fig. 14B).

Then we investigated the Raf heterodimers involved in this process by conducting dual si-RNA transfection experiment targeting three heterodimer combination. Knockdown of each heterodimer combination substantially impaired the overall SFK activation by G27 at

all infection time points indicating that all three heterodimer complexes are involved in this process (Fig. 14B).

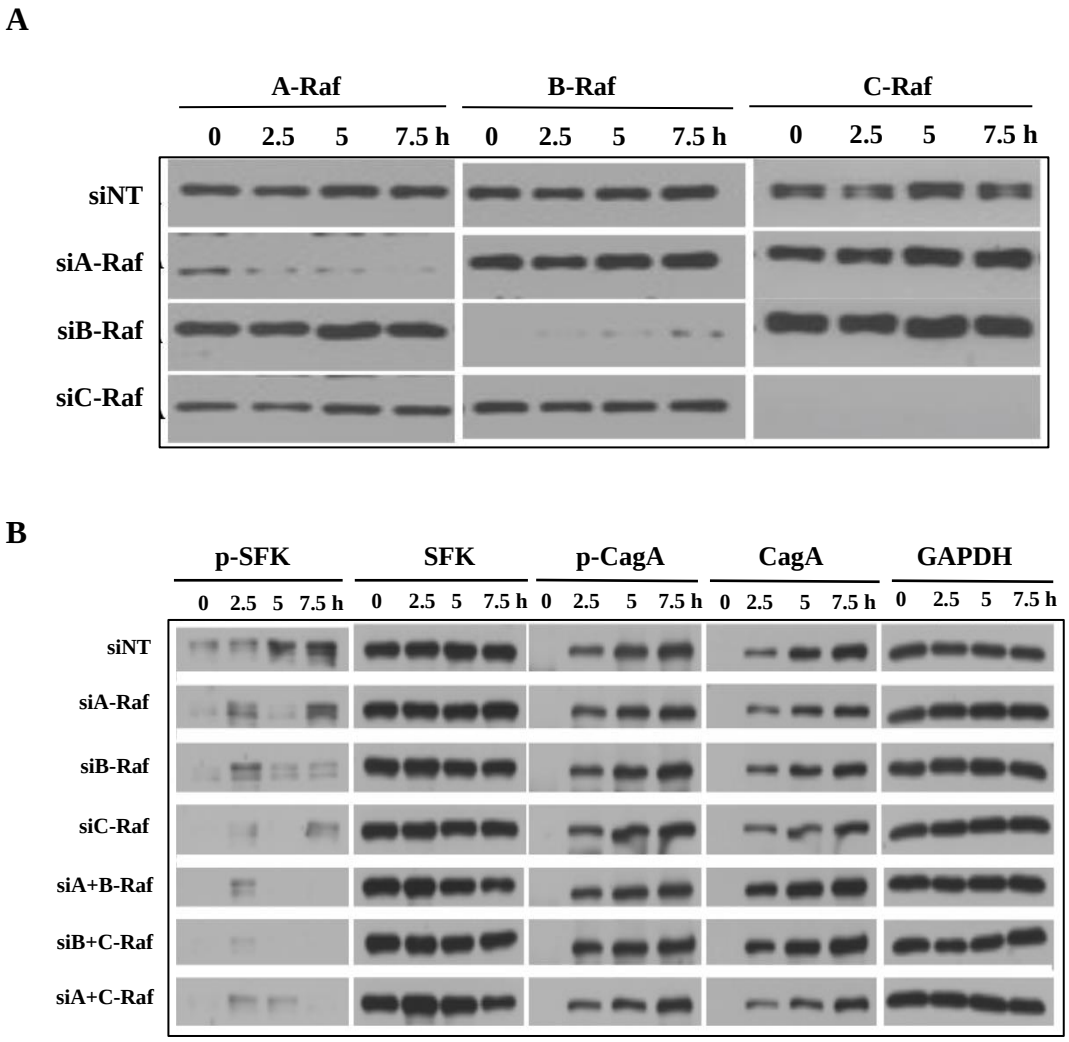

Figure 14. Effect of Raf inhibition on *H. pylori*-induced SFK activation. (A) AGS cells were transfected with 100 pM siRNA to knock down the expression of each Raf isoform. Forty-eight hours post-transfection, cells were infected (MOI-100) for different time periods, and A-Raf, B-Raf and C-Raf were immunoblotted to evaluate the expression of each Raf isoform. NT indicates the non-targeting siRNA. (B) Effect of Raf knockdown on *H. pylori*-induced SFK activation was determined by western blot.

3.2.4. Effect of Mek inhibition on *H. pylori*-induced SFK activation

As Mek is the downstream substrate of Raf, the effect of Mek inhibition on SFK activation was determined by specific siRNA knockdown. The Mek family consists of two isoforms: Mek1 and Mek2. The siRNA transfection almost entirely blocked the expression of each isoform (Fig. 15A). Knockdown of individual Mek isoforms (Mek1 or Mek2) failed to inhibit SFK activation. Interestingly, knockdown of both Mek1 and Mek2 nearly completely inhibited the SFK activation (Fig. 15B).

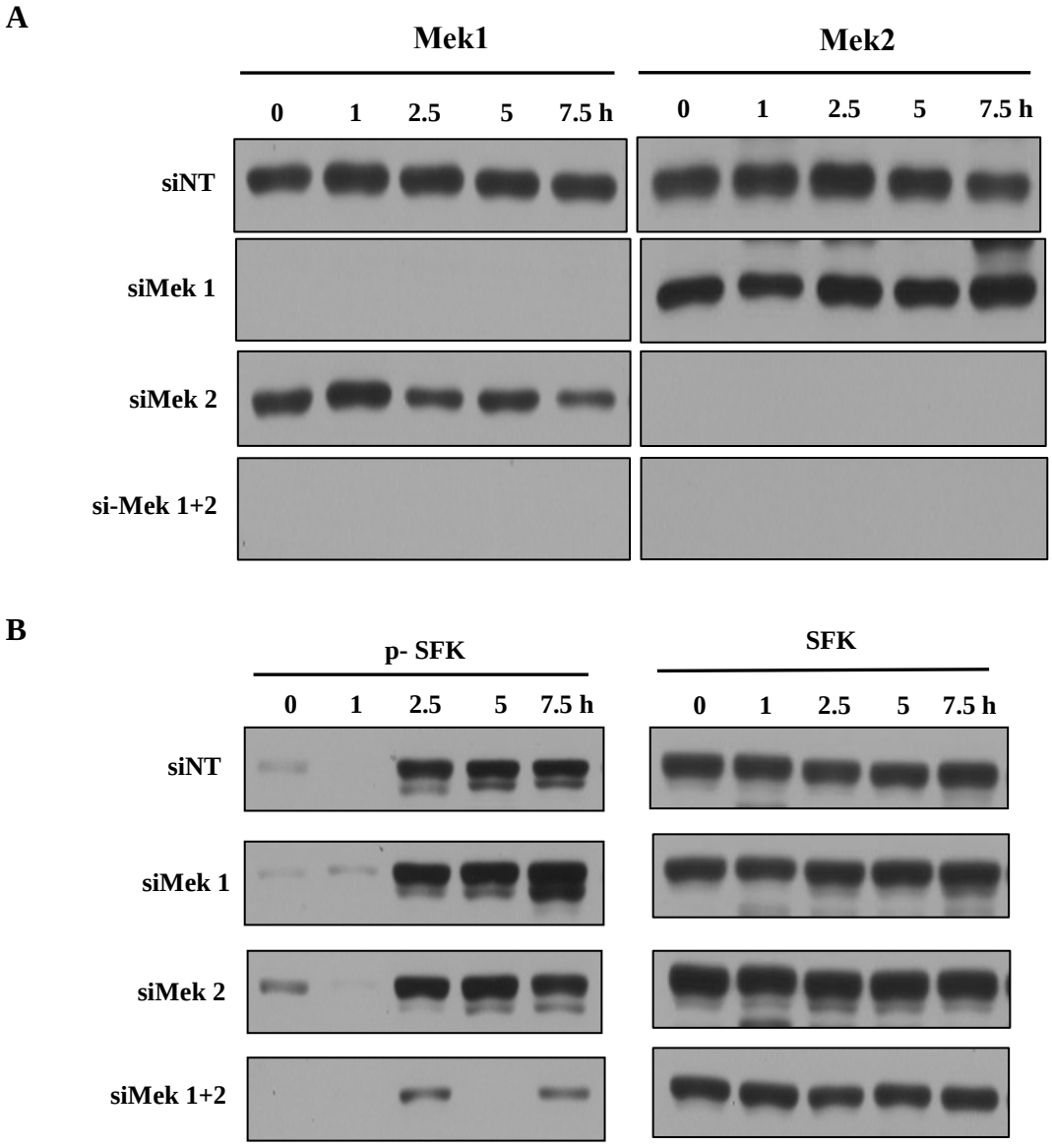

Figure 15. Effect of Mek inhibition on *H. pylori*-induced SFK activation. (A) AGS cells were transfected with 100 pM siRNA to knock down the expression of Mek1 and Mek2. Forty-eight hours post-transfection, cells were infected for different time periods, and Mek1 and Mek2 expression were determined by western blot. (B) Effect of Mek knockdown of *H. pylori*-induced SFK activation was determined by western blot.

3.2.5. Effect of Erk inhibition on *H. pylori*-induced SFK activation.

Erk is the primary downstream substrate of Mek [40]. Therefore, we determined the involvement of Erk in SFK activation by employing specific siRNA and the allosteric Mek1/2 inhibitor (CI-1040). First, we knock down the expression of Erk1 or Erk2 to determine the effect of Erk inhibition on *H. pylori*-induced SFK activation. si-RNA treatment effectively inhibits the expression of each isoform. Inhibition of either Erk1 or Erk2 expression substantially impaired SFK activation by G27 (Fig. 16A).

Then we inhibit the Erk activation using a 50 nM minimum inhibitory concentration of CI-1040. At this concentration, ERK activation was almost completely inhibited, resulting in a marked reduction in *H. pylori*-induced SFK activation. This finding suggests that ERK activation is essential for the full activation of SFKs (Fig. 16B). Collectively, these results support the conclusion that SFK activation is a downstream event of CagA phosphorylation and is likely mediated through the Shp2-ERK signaling axis.

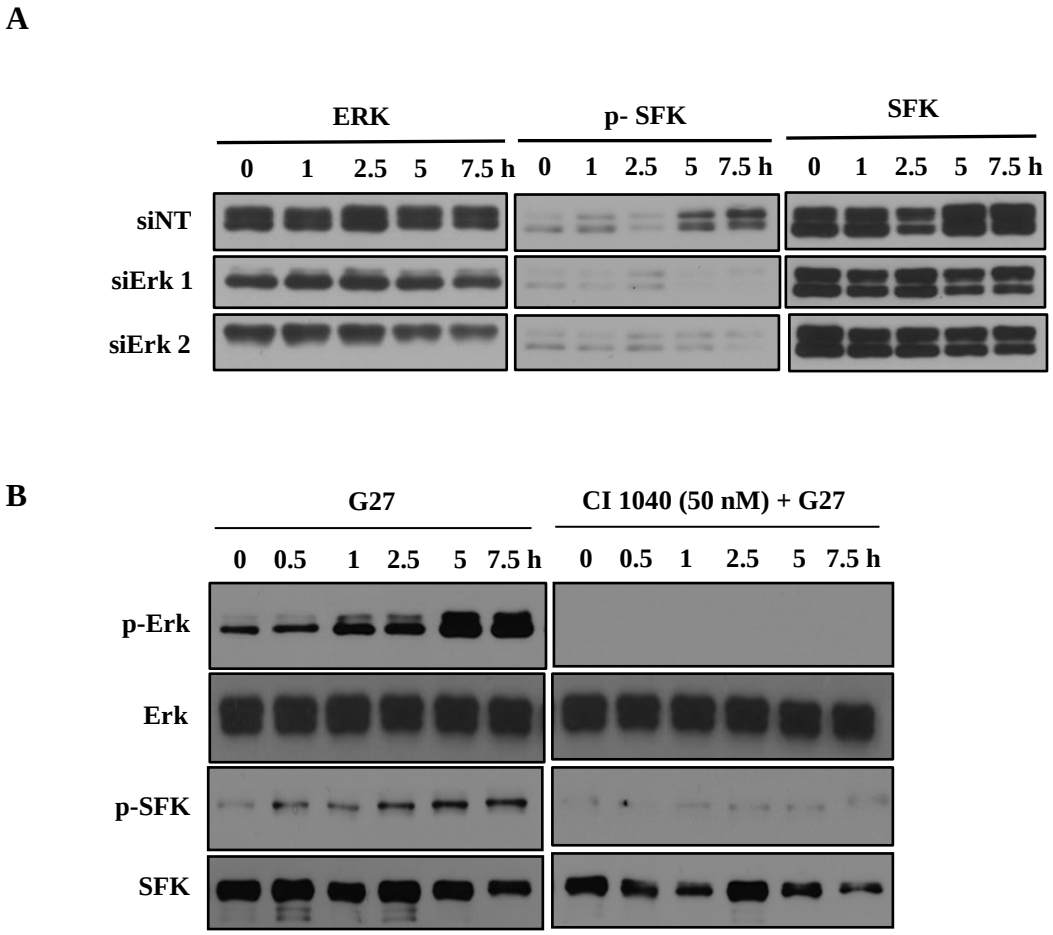

Figure 16. Effect of Erk inhibition on *H. pylori*-induced SFK activation. (A) AGS cells were transfected 100 pM siRNA to knock down the expression of Erk1 and Erk2. Forty-eight hours post-transfection, cells were infected for different time periods, and Erk 1, Erk 2, p-SFK and SFK were immunoblotted. **(B)** SFK activation was examined across multiple infection time points following pretreatment with 50 nM CI-1040 for 1 hour prior to G27 infection.

Part III

3.3.1. Effect of CagA status on AGS Cell wound healing.

To determine the impact of CagA phosphorylation status on wound healing, AGS cells were infected with G27 wild-type as well as its isogenic Δ*cagA*, G27 *cagA*-EPISA mutants for 16 hrs, and SFK activation and cell migration were evaluated. Monolayers of AGS cells were wounded and subsequently infected with *H. pylori* at a multiplicity of infection (MOI) of 100 for 16 hours. Cell migration was quantified as a ratio of the control. G27 wild-type induced significant wound healing compared to uninfected AGS cells. Wound healing induced by both Δ*cagA* and *cagA* EPISA strains was not significantly different from that of uninfected cells, nor from the wound healing induced by one another. However, the wound healing induced by the isogenic mutants was significantly lower compared to that induced by G27 wild type. SFK activation and wound healing data showed a similar trend (Fig. 17). Similar to the wound healing pattern, G27 wild type showed strong SFK activation after 16 hours of infection. The levels of SFK activation induced by both the Δ*cagA* and *cagA*-EPISA strains were similar to those in uninfected cells.

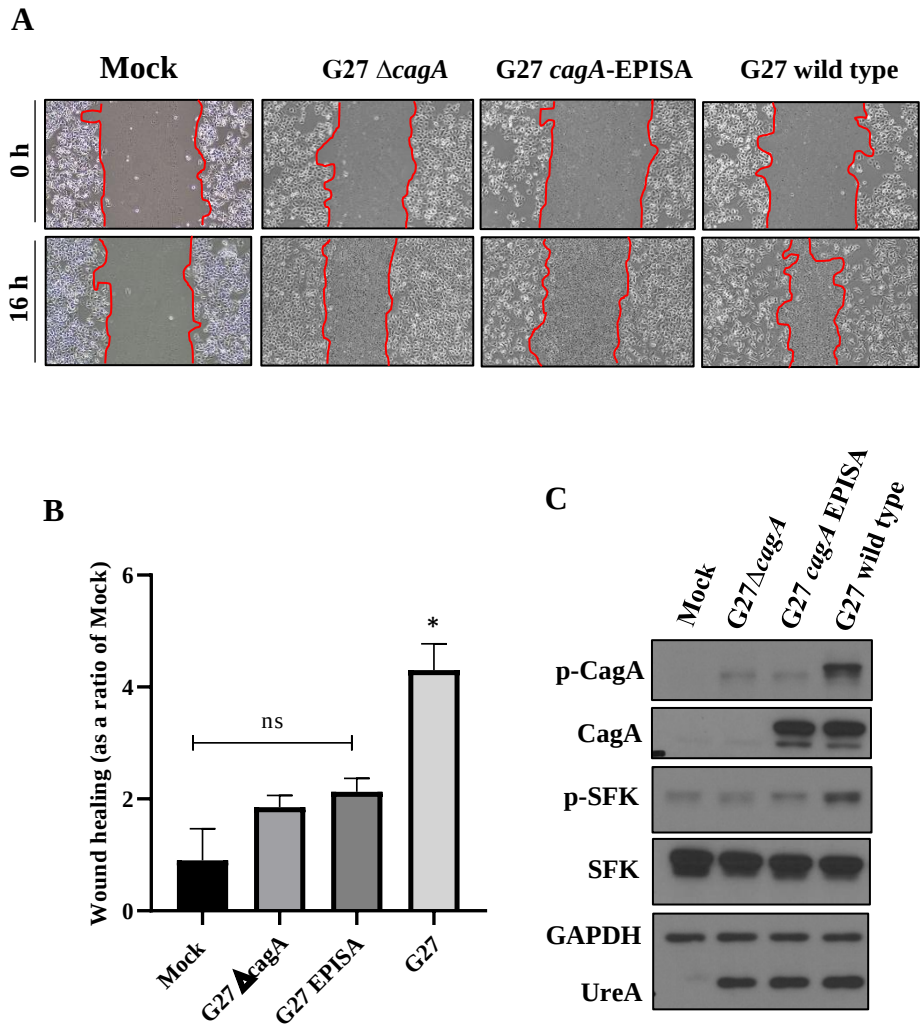

Figure 17. AGS Cell migration induced by G27 wild type and its isogenic mutants. (A) AGS cells were infected with G27 wild-type and its isogenic *cagA* mutants for 16 hours, after which the wound healing was assessed by capturing representative images. The width of the wound was measured at 0 hours and at 16 hours post-infection and, (B) The wound healing was quantified and expressed as a ratio relative to the uninfected control. Values represent the mean ± standard deviation

of three independent experiments conducted in triplicate. *P < 0.01 indicate the significant difference compared to mock. (C) SFK activation and CagA phosphorylation were analyzed by immunoblotting following 16 hours of infection.

3.3.2. Effect of CagA status on MKN28 cell wound healing.

To further validate the data obtained from the AGS cell line, MKN28 cells were infected with the cell migration were evaluated. MKN28 cell line was isolated from a patient with lymph node metastasis of gastric adenocarcinoma and has been widely used in the cell migration studies. The wound-healing assay was conducted to evaluate the cell migration. Monolayers of MKN28 cells were wounded and subsequently infected with *H. pylori* at a multiplicity of infection (MOI) of 100 for 16 hours. Cell migration was quantified as a ratio of the control. G27 wild-type induced significant (P < 0.01) wound healing compared to uninfected AGS cells. Wound healing induced by both Δ*cagA* and *cagA* EPISA strains was not significantly different from that of uninfected cells, nor from the wound healing induced by one another. Evidently, the wound healing induced by the isogenic mutants was significantly lower compared to that induced by G27 wild type. MKN28 also show a similar SFK activation and pattern to AGS cell line (Fig. 18).

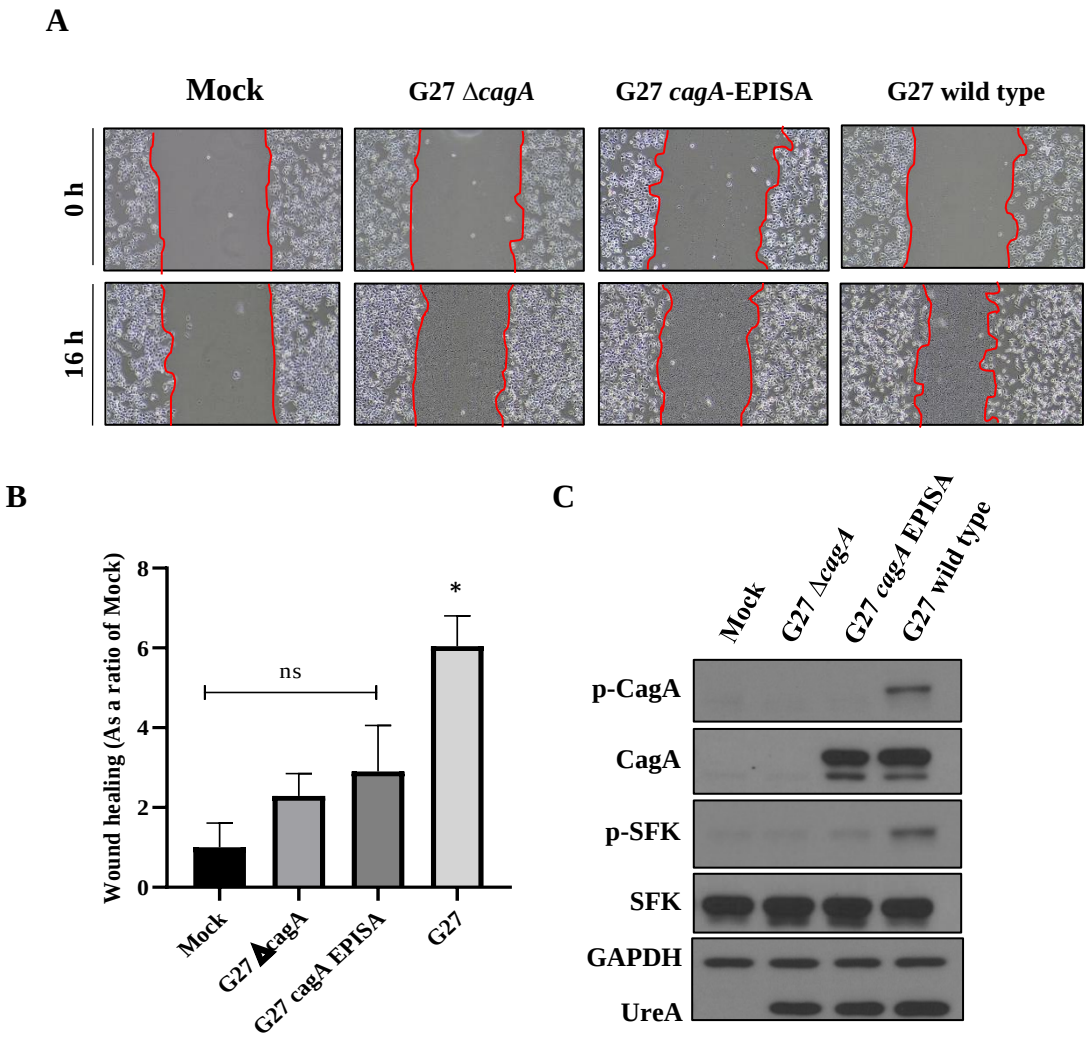

Figure 18. MKN28 Cell migration induced by G27 wild type and its isogenic mutants. (A) MKN28 cells were infected with G27 wild-type and its isogenic mutants for 16 hours, after the wound healing was assessed by capturing representative images. (B) The wound healing was quantified and expressed as a ratio relative to the uninfected control. (C) SFK activation and CagA phosphorylation were analyzed by immunoblotting following 16 hours of infection.

3.3.3. Effect of SFK inhibition on *H. pylori*-induced AGS cell wound healing.

To investigate the effect of SFK inhibition on *H. pylori*-induced AGS cell wound healing, AGS cells were subjected to wound-healing assay with or without the 0.5 μM PP2 pre-treatment, followed by G27 wild-type infection for 16 hours. G27 wild-type induce significant wound healing compared to the uninfected cells. Inhibition of SFK activation by PP2 alone did not significantly affect the basal wound healing induced by the uninfected cells. However, SFK inhibition significantly reduced the wound healing induced by the *H. pylori* infection indicating that the SFK activation is crucial to mediate the *H. pylori* induce cell migration (Fig. 19).

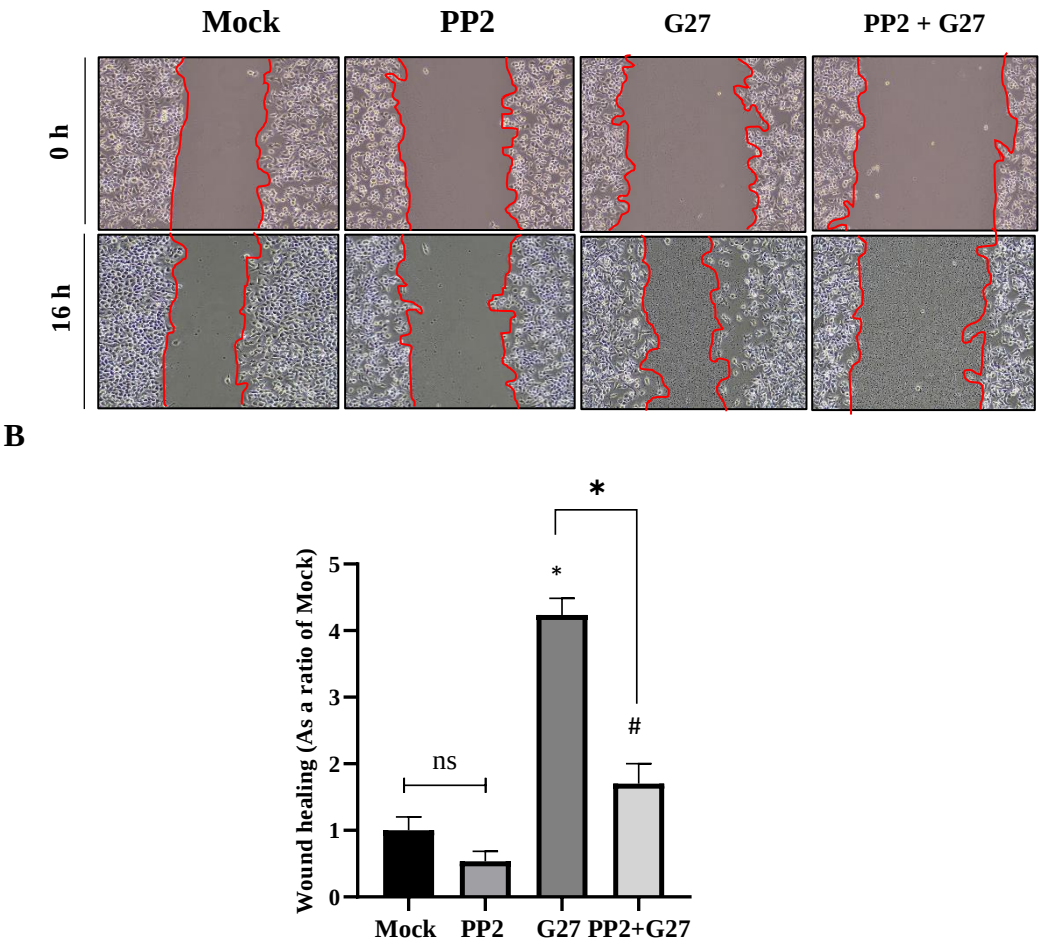

Figure 19. Effect of SFK inhibition on AGS cell migration. AGS cells were pretreated with 0.5 μM PP2 and subsequently infected with G27 wild-type for 16 hours. Representative images (A) were captured and, (B) cell migration was quantified and expressed as a ratio relative to the uninfected control (*P < 0.01; #P < 0.01). The values represent the mean ± standard deviation of three independent experiments conducted in triplicate.

3.3.4. Effect of SFK inhibition on MKN28 cell wound healing.

Next, we determined the effect of SFK inhibition on *H. pylori*-induced MKN28 cell migration. The cells were subjected to a wound-healing assay with or without the 0.5 μM PP2 pre-treatment, followed by infection with wild-type G27 for 16 hours. Aligning with the pattern observed in AGS cell line, the G27 wild-type shows significant wound healing compared to uninfected cells. Also, the SFK inhibition alone did not significantly impair the healing of the basal wound by uninfected cells. However, the SFK inhibition significantly impaired the wound healing induced by G27, further supporting the idea that SFK activation is a crucial mediator of *H. pylori*-induced wound healing (Fig. 20).

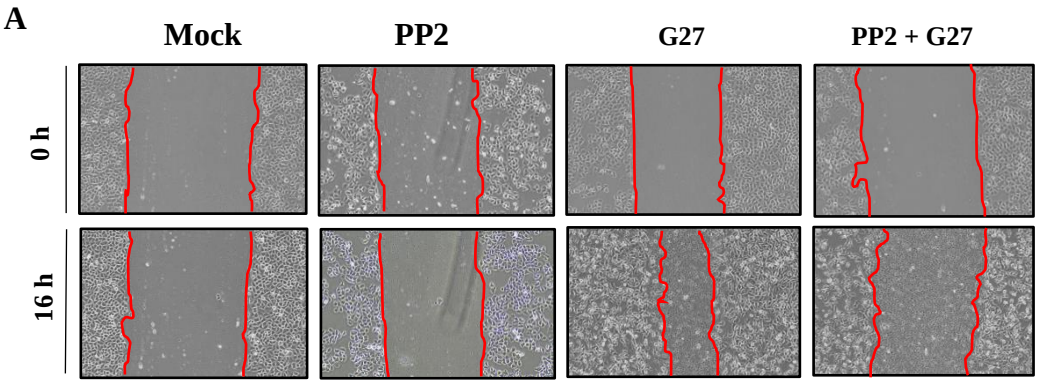

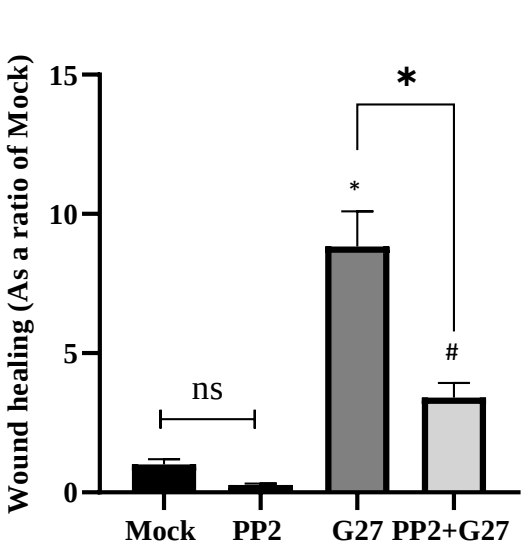

Figure 20. Effect of SFK inhibition on MKN28 cell migration. MKN28 cells were pretreated with or without PP2 and subsequently infected with G27 wild-type for 16 hours. Representative images were captured (A) and the wound healing (B) was quantified and expressed as a ratio relative to the uninfected control. *$P < 0.01$; #$P < 0.05$

3.3.5. Effect of SFK inhibition on AGS cell invasion

To examine the impact of SFK inhibition on *H. pylori*-induced cell invasion, AGS cells were subjected to a Matrigel-coated Transwell invasion assay with or without 0.5 μM PP2 treatment followed by infection with wild-type G27 for 16 hours. Infection with G27 significantly (*$P < 0.01$) enhanced AGS cell invasion compared to uninfected controls, indicating the bacteria's strong pro-invasive potential. Importantly, SFK inhibition alone did not affect the cell invasion of uninfected cells, suggesting that SFKs are not essential for the basal invasion under normal conditions. In contrast, PP2 treatment markedly suppressed the *H. pylori*-induced increase in invasion, demonstrating that SFK activity is specifically required for the bacterium-driven invasive response (Fig. 21). These findings collectively indicate that SFK activation is a critical mediator of *H. pylori*-induced AGS cell invasion.

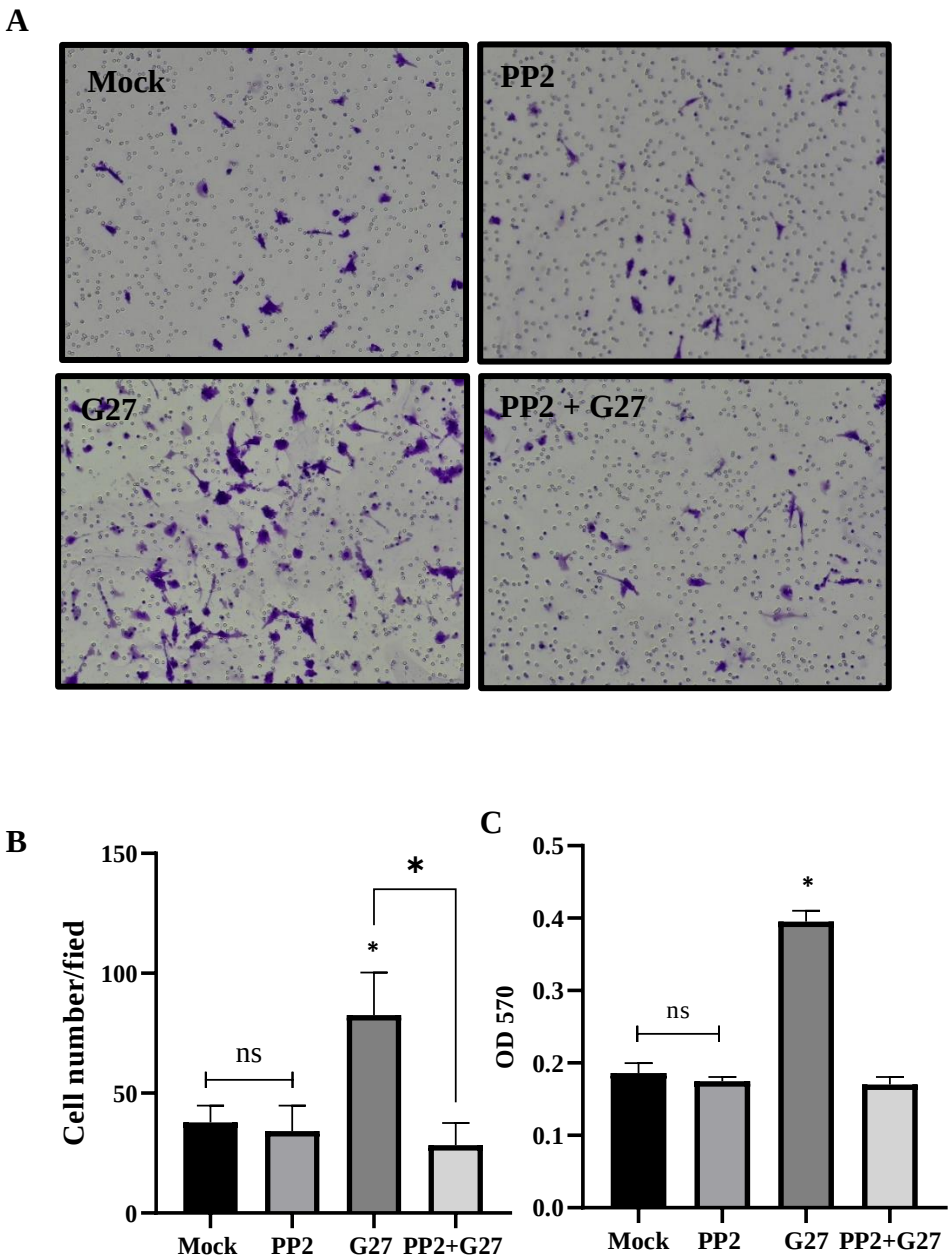

Figure 21. Effect of SFK inhibition on AGS cell invasion. Transwell matrigel invasion assay was performed using 12-well Transwell inserts. The insert was coated with the 1:10 diluted matrigel, and cells were seeded onto the solidified matrigel with or without PP2. Five hours after seeding, cells were infected with *H. pylori* for 16 hours, and the invaded cells were fixed, stained, and quantified using ImageJ software. (A) Representative images are shown, and cell invasion was quantified as the number of invaded cells per field (B) and by (C) measuring the total number of invaded cells through DMSO lysis. The values represent the mean ± standard deviation of three independent experiments conducted in triplicate.

3.3.6. Effect of SFK inhibition on MKN28 cell invasion.

To further supplement the data obtained from the AGS cell line, Next, MKN28 cells were subjected to a transwell Matrigel invasion assay with or without pre-treatment using 0.5 μM PP2, a selective SFK inhibitor, followed by infection with wild-type *H. pylori* strain G27 for 16 hours. Consistent with the pattern observed in the AGS cell line, infection with G27 significantly enhanced ($^{*}P < 0.01$) MKN28 cell invasion compared to uninfected controls. Furthermore, SFK inhibition alone did not significantly affect the basal cell invasion of uninfected cells. In contrast, PP2 treatment markedly suppressed the *H. pylori*-induced increase in invasion, demonstrating that SFK activity is specifically required for the bacterium-driven invasive response (Fig. 22).

A

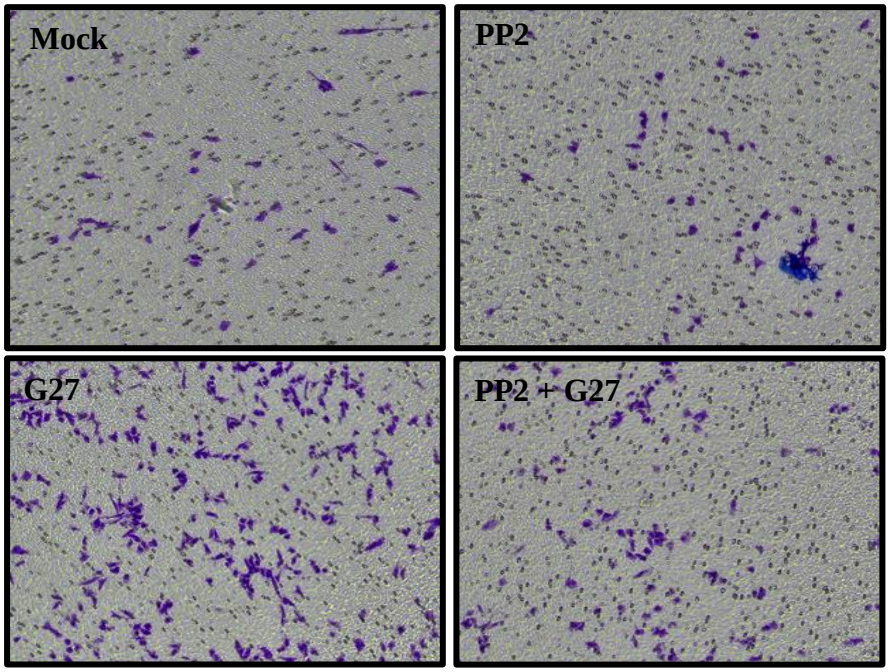

B

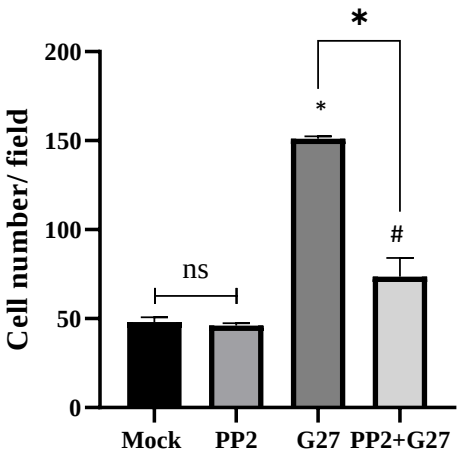

C

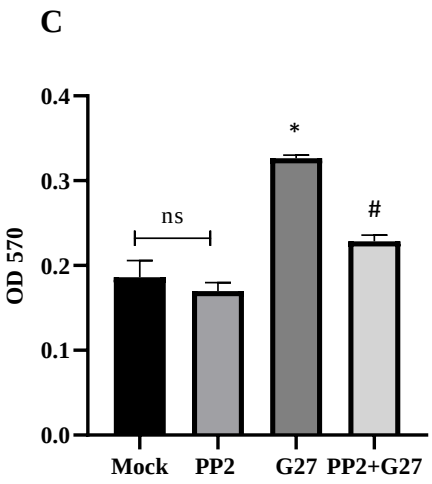

Figure 22. Effect of SFK inhibition on MKN28 cell invasion. Transwell matrigel invasion assay was performed using 12-well Transwell inserts. The insert was coated with the diluted metrigel, and cells were seeded onto the solidified matrigel with or without PP2. Five hours after seeding, cells were infected with *H. pylori* for 16 hours, and the invaded cells were fixed, stained, and quantified using Image J software. (A) Representative images are shown, and cell invasion was quantified as the number of invaded cells per field (B) and by (C) measuring the total number of invaded cells through DMSO lysis. # indicate the significance ($P < 0.01$) compared to PP2.

4. Discussion

The current work investigated the role of Src Family Kinases (SFKs) in *Helicobacter pylori*-mediated CagA phosphorylation and the resulting cellular phenotypes, including cell elongation, IL-8 secretion, and cell migration. Although SFKs have been widely regarded as the principal kinases responsible for CagA phosphorylation [21,22], our findings challenge this long-standing view by demonstrating that SFK activation is not essential for CagA phosphorylation or its canonical downstream effects.

Using the selective SFK inhibitor PP2, we observed complete inhibition of SFK activation at 0.5 μM without a significant reduction in phosphorylation of CagA, cell elongation, or IL-8 induction. Using this minimum inhibitory concentration, we suggest that CagA phosphorylation can proceed independently of SFK activity in gastric epithelial cells, implicating the involvement of alternative host kinases. Previous studies have suggested that kinases such as Abl may also contribute to CagA phosphorylation in an EPIYA-specific and time-dependent manner [41]. Although it is not widely appreciated, it is also suggested that EGFR receptor tyrosine kinase may be involved in this process [10]. Based on the recent study, we further emphasize the need to reevaluate the kinases involved in CagA phosphorylation.

Interestingly, higher concentrations of PP2 led to a dose-dependent decrease in both CagA phosphorylation and cell elongation. However, immunofluorescence and FACS analyses revealed that these effects coincided with a reduction in bacterial binding to AGS cells.

Therefore, it is likely that the observed decrease in CagA activity at higher PP2 concentrations is a consequence of reduced *H. pylori* attachment rather than direct inhibition of SFK activation. This phenomenon is highly overlooked in previously reported studies where considerably high PP2 concentrations have been used to achieve SFK inhibition. It is widely known that pharmacological inhibitors exhibit off-target effects at concentrations beyond the optimum [42]. Although our study lacks direct evidence for the mechanism behind this, it is likely a result of off-target inhibitory effects on host cell molecules mediating bacterial attachment.

We employed infections with a Δ*cagA* mutant and a phosphorylation-resistant *cagA*-EPISA mutant to dissect the signaling cascade further. Both strains failed to induce SFK activation, strongly suggesting that SFK activation predominantly occurs downstream of CagA phosphorylation. This finding not only reinforces that SFK activation is not required for CagA phosphorylation but also suggests the involvement of an alternative signaling pathway that drives SFK activation during *H. pylori* infection. Although SFK activation is widely addressed upstream of Erk pathway activation [20], SFK inhibition by PP2 did not impair ERK activation, suggesting that the ERK pathway acts independently of SFK activation. Our subsequent experiments, using siRNA and Mek inhibitor, revealed that the Shp2-Raf-Mek-Erk axis mediates this activation, positioning the ERK pathway as an upstream regulator of SFK activation during *H. pylori* infection.

Interestingly, SFK activation appeared to be influenced by all key molecules within the ERK signaling cascade. Knockdown of each Raf isoform had differential effects on SFK

activation where B-Raf and C-Raf showed predominant effects on *H. pylori*-induced SFK activation. Yet, all three isoforms were differentially involved in SFK activation in different infection times, showcasing the complex interplay of Raf family members in SFK activation. Inhibition of either MEK1 or MEK2 alone had little effect on SFK activation, whereas simultaneous inhibition of both isoforms nearly abolished it. This suggests that MEK1 and MEK2 play redundant roles in SFK activation, likely compensating for each other when one is inhibited. In contrast, inhibition of either ERK1 or ERK2 significantly impaired SFK activation, suggesting that ERK heterodimer formation is essential for transmitting the SFK activation signal during *H. pylori* infection.

While SFKs were dispensable for early *H. pylori*-mediated responses such as elongation of cells and secretion of IL-8, our study provides compelling evidence that SFK activation is a primary mediator of infection driven gastric epithelial cell motility. Using wound-healing assays, we found that infection with wild-type G27 significantly enhanced cell migration in both AGS and MKN28 cells, whereas the Δ*cagA* and *cagA*-EPISA mutants failed to promote migration, displaying levels comparable to uninfected controls. This indicates that CagA phosphorylation is essential for the migratory response. The same trend was observed in SFK activation, where only the wild-type strain induced strong phosphorylation. Pre-treatment with PP2 significantly impaired *H. pylori*-induced migration but it showed no impact on the inherent migratory activity of uninfected cells. These results were consistent across both cell lines, reinforcing the specificity of SFK activation in infection-driven motility. Similar findings were observed in the Matrigel

invasion assay, where G27 infection promoted a strong invasive phenotype that was significantly impaired by PP2 treatment. Again, SFK inhibition did not affect the basal invasion of uninfected cells, suggesting that SFKs are dispensable under normal conditions but essential for *H. pylori*-driven responses.

Taken together, our findings redefine the role of Src Family Kinases (SFKs) in *H. pylori* pathogenesis by demonstrating that SFK activation is dispensable for CagA phosphorylation, cell elongation, and IL-8 induction, but is critically required for *H. pylori*-induced gastric epithelial cell migration and invasion. We demonstrate that CagA phosphorylation proceeds independently of SFKs and, instead, SFK activation occurs downstream via the Shp2-Raf-MEK-ERK signaling cascade. These insights revise the conventional model of CagA-SFK signaling and highlight a previously underappreciated signaling hierarchy in which ERK activation governs infection-driven SFK activation and motility-related phenotypes. By clarifying the molecular basis of *H. pylori*-induced epithelial migration and invasion, this study contributes to a deeper mechanistic understanding of bacterial virulence strategies. It may inform the development of targeted interventions to disrupt *H. pylori*-associated gastric disease progression.

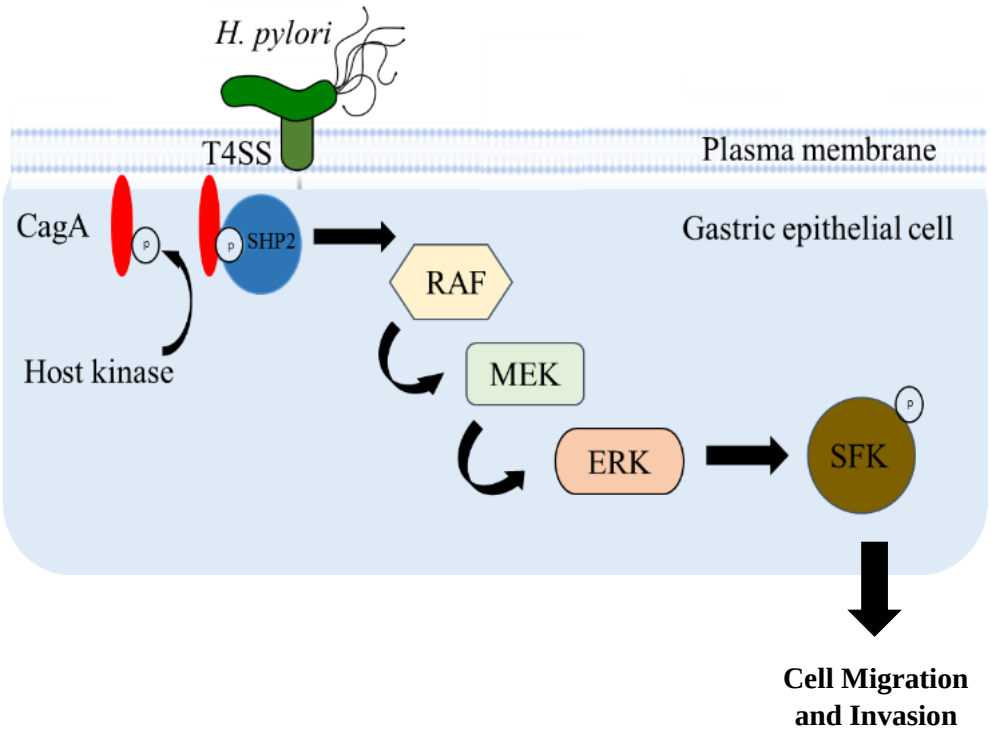

Figure 23. Schematic summary of key findings. *Helicobacter pylori* translocate CagA into gastric epithelial cells via the type IV secretion system and undergoes phosphorylation by host cell kinases. Once phosphorylated, CagA deregulates Shp2 and activates the Erk pathway, which in turn activates SFKs in response to *H. pylori* infection. Shp2, Raf, Mek, and Erk are involved in the SFK activation signal downstream of CagA phosphorylation. SFK activation appears to be dispensable for CagA phosphorylation, cell elongation, and IL-8 induction. However, SFK activation in response to *H. pylori* infection is crucial to drive cell migration and invasion induced by *H. pylori* infection.

6. Reference list

1 Polk, D. B. & Peek, R. M., Jr. *Helicobacter pylori*: gastric cancer and beyond. *Nat Rev Cancer* **10**, 403-414, doi:10.1038/nrc2857 (2010).

2 Thrift, A. P., Wenker, T. N. & El-Serag, H. B. Global burden of gastric cancer: epidemiological trends, risk factors, screening and prevention. *Nature Reviews Clinical Oncology* **20**, 338-349, doi:10.1038/s41571-023-00747-0 (2023).

3 Chen, Y.-C. *et al.* Global Prevalence of *Helicobacter pylori* Infection and Incidence of Gastric Cancer Between 1980 and 2022. *Gastroenterology* **166**, 605-619, doi:https:10.1053/j.gastro.2023.12.022 (2024).

4 Ernst, P. B. & Gold, B. D. The disease spectrum of *Helicobacter pylori*: the immunopathogenesis of gastroduodenal ulcer and gastric cancer. *Annu Rev Microbiol* **54**, 615-640, doi:10.1146/annurev.micro.54.1.615 (2000).

5 Peek, R. M., Jr. & Crabtree, J. E. *Helicobacter* infection and gastric neoplasia. *J Pathol* **208**, 233-248, doi:10.1002/path.1868 (2006).

6 Ferlay, J. *et al.* Cancer incidence and mortality worldwide: sources, methods and major patterns in GLOBOCAN 2012. *Int J Cancer* **136**, E359-386, doi:10.1002/ijc.29210 (2015).

7 Salvatori, S., Marafini, I., Laudisi, F., Monteleone, G. & Stolfi, C. *Helicobacter pylori* and Gastric Cancer: Pathogenetic Mechanisms. *Int J Mol Sci* **24**, doi:10.3390/ijms24032895 (2023).

8 Schistosomes, liver flukes and *Helicobacter pylori*. *IARC Monogr Eval Carcinog Risks Hum* **61**, 1-241 (1994).

9 Odenbreit, S. *et al.* Translocation of *Helicobacter pylori* CagA into gastric epithelial cells by type IV secretion. *Science* **287**, 1497-1500, doi:10.1126/science.287.5457.1497 (2000).

10 Asahi, M. *et al. Helicobacter pylori* CagA protein can be tyrosine phosphorylated in gastric epithelial cells. *J Exp Med* **191**, 593-602, doi:10.1084/jem.191.4.593 (2000).

11 Stein, M., Rappuoli, R. & Covacci, A. Tyrosine phosphorylation of the *Helicobacter pylori* CagA antigen after *cag*-driven host cell translocation. *Proc Natl Acad Sci U S A* **97**, 1263-1268, doi:10.1073/pnas.97.3.1263 (2000).

12 Higashi, H. *et al.* SHP-2 tyrosine phosphatase as an intracellular target of *Helicobacter pylori* CagA protein. *Science* **295**, 683-686, doi:10.1126/science.1067147 (2002).

13 Neel, B. G., Gu, H. & Pao, L. The 'Shp'ing news: SH2 domain-containing tyrosine phosphatases in cell signaling. *Trends Biochem Sci* **28**, 284-293, doi:10.1016/s0968-0004(03)00091-4 (2003).

14 Backert, S., Moese, S., Selbach, M., Brinkmann, V. & Meyer, T. F. Phosphorylation of tyrosine 972 of the *Helicobacter pylori* CagA protein is essential for induction of a scattering phenotype in gastric epithelial cells. *Mol Microbiol* **42**, 631-644, doi:10.1046/j.1365-2958.2001.02649.x (2001).

15 Tegtmeyer, N. *et al.* Importance of EGF receptor, HER2/Neu and Erk1/2 kinase signalling for host cell elongation and scattering induced by the *Helicobacter pylori* CagA protein: antagonistic effects of the vacuolating cytotoxin VacA. *Cell Microbiol* **11**, 488-505, doi:10.1111/j.1462-5822.2008.01269.x (2009).

16 Allison, C. C., Kufer, T. A., Kremmer, E., Kaparakis, M. & Ferrero, R. L. *Helicobacter pylori* induces MAPK phosphorylation and AP-1 activation via a NOD1-dependent mechanism. *J Immunol* **183**, 8099-8109, doi:10.4049/jimmunol.0900664 (2009).

17 Jang, S., Kim, J. & Cha, J. H. Cot kinase plays a critical role in *Helicobacter pylori*-induced IL-8 expression. *J Microbiol* **55**, 311-317, doi:10.1007/s12275-017-7052-9 (2017).

18 Segal, E. D., Cha, J., Lo, J., Falkow, S. & Tompkins, L. S. Altered states: involvement of phosphorylated CagA in the induction of host cellular growth changes by *Helicobacter pylori*. *Proc Natl Acad Sci U S A* **96**, 14559-14564, doi:10.1073/pnas.96.25.14559 (1999).

19 Higashi, H. *et al.* Biological activity of the *Helicobacter pylori* virulence factor CagA is determined by variation in the tyrosine phosphorylation sites. *Proc Natl Acad Sci U S A* **99**, 14428-14433, doi:10.1073/pnas.222375399 (2002).

20 Higashi, H. *et al. Helicobacter pylori* CagA induces Ras-independent morphogenetic response through SHP-2 recruitment and activation. *J Biol Chem* **279**, 17205-17216, doi:10.1074/jbc.M309964200 (2004).

21 Selbach, M., Moese, S., Hauck, C. R., Meyer, T. F. & Backert, S. Src is the kinase of the *Helicobacter pylori* CagA protein in vitro and in vivo. *J Biol Chem* **277**, 6775-6778, doi:10.1074/jbc.C100754200 (2002).

22 Stein, M. *et al.* c-Src/Lyn kinases activate *Helicobacter pylori* CagA through tyrosine phosphorylation of the EPIYA motifs. *Mol Microbiol* **43**, 971-980, doi:10.1046/j.1365-2958.2002.02781.x (2002).

23 Roskoski, R., Jr. Src kinase regulation by phosphorylation and dephosphorylation. *Biochem Biophys Res Commun* **331**, 1-14, doi:10.1016/j.bbrc.2005.03.012 (2005).

24 Wessler, S., Gimona, M. & Rieder, G. Regulation of the actin cytoskeleton in *Helicobacter pylori*-induced migration and invasive growth of gastric epithelial cells. *Cell Communication and Signaling* **9**, 27, doi:10.1186/1478-811X-9-27 (2011).

25 Tabassam, F. H., Graham, D. Y. & Yamaoka, Y. Paxillin is a novel cellular target for converging *Helicobacter pylori*-induced cellular signaling. *Am J Physiol Gastrointest Liver Physiol* **301**, G601-611, doi:10.1152/ajpgi.00375.2010 (2011).

26 Costa, A. M. *et al. Helicobacter pylori* Activates Matrix Metalloproteinase 10 in Gastric Epithelial Cells via EGFR and ERK-mediated Pathways. *The Journal of Infectious Diseases* **213**, 1767-1776, doi:10.1093/infdis/jiw031 (2016).

27 Xiang, Z. *et al.* Analysis of expression of CagA and VacA virulence factors in 43 strains of *Helicobacter pylori* reveals that clinical isolates can be divided into two

major types and that CagA is not necessary for expression of the vacuolating cytotoxin. *Infect Immun* **63**, 94-98, doi:10.1128/iai.63.1.94-98.1995 (1995).

28 Covacci, A. *et al.* Molecular characterization of the 128-kDa immunodominant antigen of *Helicobacter pylori* associated with cytotoxicity and duodenal ulcer. *Proc Natl Acad Sci U S A* **90**, 5791-5795, doi:10.1073/pnas.90.12.5791 (1993).

29 Baltrus, D. A. *et al.* The complete genome sequence of *Helicobacter pylori* strain G27. *J Bacteriol* **191**, 447-448, doi:10.1128/jb.01416-08 (2009).

30 Jones, K. R. *et al.* Polymorphism in the CagA EPIYA motif impacts development of gastric cancer. *J Clin Microbiol* **47**, 959-968, doi:10.1128/jcm.02330-08 (2009).

31 Gunawardhana, N. *et al. Helicobacter pylori*-Induced HB-EGF Upregulates Gastrin Expression via the EGF Receptor, C-Raf, Mek1, and Erk2 in the MAPK Pathway. *Front Cell Infect Microbiol* **7**, 541, doi:10.3389/fcimb.2017.00541 (2017).

32 Busuttil, R. A. *et al.* An orthotopic mouse model of gastric cancer invasion and metastasis. *Scientific Reports* **8**, 825, doi:10.1038/s41598-017-19025-y (2018).

33 Moese, S. *et al. Helicobacter pylori* induces AGS cell motility and elongation via independent signaling pathways. *Infect Immun* **72**, 3646-3649, doi:10.1128/iai.72.6.3646-3649.2004 (2004).

34 Kwok, T. *et al. Helicobacter* exploits integrin for type IV secretion and kinase activation. *Nature* **449**, 862-866, doi:10.1038/nature06187 (2007).

35 Eftang, L. L., Esbensen, Y., Tannæs, T. M., Bukholm, I. R. & Bukholm, G. Interleukin-8 is the single most up-regulated gene in whole genome profiling of *H. pylori* exposed gastric epithelial cells. *BMC Microbiol* **12**, 9, doi:10.1186/1471-2180-12-9 (2012).

36 Brandt, S., Kwok, T., Hartig, R., König, W. & Backert, S. NF-kappaB activation and potentiation of proinflammatory responses by the *Helicobacter pylori* CagA protein. *Proc Natl Acad Sci U S A* **102**, 9300-9305, doi:10.1073/pnas.0409873102 (2005).

37 Kim, S. Y., Lee, Y. C., Kim, H. K. & Blaser, M. J. *Helicobacter pylori* CagA transfection of gastric epithelial cells induces interleukin-8. *Cell Microbiol* **8**, 97-106, doi:10.1111/j.1462-5822.2005.00603.x (2006).

38 Hayashi, T. *et al.* Differential Mechanisms for SHP2 Binding and Activation Are Exploited by Geographically Distinct *Helicobacter pylori* CagA Oncoproteins. *Cell Reports* **20**, 2876-2890, doi:10.1016/j.celrep.2017.08.080 (2017).

39 Lee, I. O. *et al. Helicobacter pylori* CagA phosphorylation status determines the gp130-activated SHP2/ERK and JAK/STAT signal transduction pathways in gastric epithelial cells. *J Biol Chem* **285**, 16042-16050, doi:10.1074/jbc.M110.111054 (2010).

40 Crews, C. M. & Erikson, R. L. Purification of a murine protein-tyrosine/threonine kinase that phosphorylates and activates the Erk-1 gene product: relationship to the

fission yeast byr1 gene product. *Proc Natl Acad Sci U S A* **89**, 8205-8209, doi:10.1073/pnas.89.17.8205 (1992).

41 Mueller, D. *et al.* c-Src and c-Abl kinases control hierarchic phosphorylation and function of the CagA effector protein in Western and East Asian *Helicobacter pylori* strains. *J Clin Invest* **122**, 1553-1566, doi:10.1172/jci61143 (2012).

42 Lo, Y. C. *et al.* Computational analysis of kinase inhibitor selectivity using structural knowledge. *Bioinformatics* **35**, 235-242, doi:10.1093/bioinformatics/bty582 (2019).

7. Abstract (Korean)

헬리코박터 파일로리 감염에서 CagA 인산화 후 새롭게 규명된 하위 신호인 SFK 활성화의 기능적 역할 규명

지도교수 차정헌

연세대학교 대학원 응용생명과학과

Ramanayake Mudiyanselage Ashansa Pamodhi Ramanayake

헬리코박터 파일로리 감염에서 CagA 인산화 후 새롭게 규명된 하위 신호인 SFK 활성화의 기능적 역할 규명

Helicobacter pylori 는 위암과 소화성 궤양의 발생과 밀접하게 관련된 위장 병원균이다. 이 균의 주요 병원성 인자 중 하나인 종양단백질 CagA 는 제 4 형 분비 체계을 통해 위 상피세포 내로 주입되며, 세포 내에서 티로신 인산화 과정을 거쳐 다양한 세포 신호 전달 경로를 활성화시키고 세포신장 (Humminbird phenotype) 을 유도한다. CagA 인산화에 관여하는 주요 인산화효소로 Src 계열 인산화효소(SFK)가 알려져 있으나, 본 연구에서는 CagA 인산화, SFK 활성화, 그리고 이로 인한 세포 반응 간의 연관성을 재평가하였다.

SFK 가 CagA 인산화 및 *H. pylori*-매개 세포 신장에 어떤 역할을 하는지를 분석하기 위해 SFK 억제제인 PP2 를 이용하였다. SFK 활성화 및 CagA 인산화 여부는 immunoblotting 을 통해 분석하였고, 세포 신장 여부는 현미경 관찰을 통해 평가하였다. 또한, *H. pylori* 의 AGS 세포 부착 능력은 Immunofluorescence assay 과 FACS 분석을 통해 측정하였다. SFK 활성화와 CagA 인산화 간의 관계를 명확히 하기 위해, *cagA* 유전자 결손 균주(Δ*cagA*) 및 인산화 저항성 *cagA* 돌연변이 균주(*cagA*-EPISA) 감염도 함께 수행하였다.

연구 결과, 0.5 μM 농도의 PP2 처리 시 SFK 활성화는 완전히 억제되었으나, CagA 인산화, 세포 신장, IL-8 생성에는 큰 영향을 미치지 않았다. 이는 SFK 가 이러한 과정에 필수적이지 않음을 시사한다. 그러나 PP2 농도가 증가함에 따라 CagA 인산화 및 세포 신장은 농도 의존적으로 감소하였다. Immunofluorescence assay 및 FACS 분석 결과, PP2 처리로 인해 *H. pylori* 의 AGS 세포 부착 능력이 감소한 것으로 나타났다. Δ*cagA* 및 *cagA*-EPISA 균주에 의한 감염은 SFK 를 활성화하지 못하였으며, 이는 SFK 활성화가 CagA 인산화 이후 단계에서 발생함을 시사한다. 추가로, 특정 siRNA 와 억제제를 사용한 실험을 통해, *H. pylori*-매개 SFK 활성화가 Shp2–Raf–Mek–Erk 신호 경로를 통해 조절됨을 확인하였다.

또한, SFK 억제는 ERK 활성화 및 IL-8 생성에는 영향을 미치지 않았지만, wound healing assay 와 transwell invasion assay 에서는 *H. pylori* 감염에 따른 세포 이동성과 침습성이 크게 감소하였다. 이는 감염 과정에서 SFK 가 숙주 세포 이동성 조절에 중요한 역할을 한다는 점을 보여준다.

본 연구는 CagA 인산화를 매개하는 주된 키나아제가 SFK 라는 기존 관점을 재고하게 한다. 오히려 SFK 는 CagA 인산화 이후 ERK 경로를 통해 활성화될 수 있으며, CagA 인산화는 다른 키나아제에 의해 매개될 가능성을 제시한다. SFK 는 CagA 인산화, ERK 활성화, 세포 신장, IL-8 생성에는 필수적이지 않았지만, *H. pylori* 감염에 따른 세포 이동 및 침습에는 결정적인 역할을 수행하였다. 이 연구는 감염 과정에서 SFK 가 숙주 세포 이동성을 조절하는 데 있어 필수적이며, 지금까지 간과되었던 그 역할을 새롭게 평가한 것이다.

헬리코박터 파일로리, SFK 활성화, CagA 인산화, 세포 신장, IL-8 유도, SHP2, RAF, MEK, ERK, 세포 이동 및 침습